

Institutionen för fysik, kemi och biologi

Examensarbete

**Combining Reflectometry, Ablation and Fluid
Collection in a Microstructured Fiber**

Azizahalhakim Sudirman
Examensarbetet utfört vid Acreo AB
Linköping 2009

LITH-IFM-A-EX--09/2065—SE



TEKNISKA HÖGSKOLAN
LINKÖPINGS UNIVERSITET

Linköpings universitet Institutionen för fysik, kemi och biologi
581 83 Linköping

Institutionen för fysik, kemi och biologi

**Combining Reflectometry, Ablation and Fluid
Collection in a Microstructured Fiber**

Azizahhakim Sudirman

Examensarbetet utfört vid Acreo AB

Linköping 2009

Handledare

Walter Margulis, Acreo AB

Examinator

Hans Arwin, IFM, Linköpings Universitet



TEKNISKA HÖGSKOLAN
LINKÖPINGS UNIVERSITET



Avdelning, institution
Division, Department

Chemistry
Department of Physics, Chemistry and Biology
Linköping University

Datum

Date

2009-09-22

Språk

Language

- Svenska/Swedish
 Engelska/English

Rapporttyp

Report category

- Licentiatavhandling
 Examensarbete
 C-uppsats
 D-uppsats
 Övrig rapport

ISBN

ISRN: LITH-IFM-A-EX--09/2065--SE

Serietitel och serienummer

ISSN

Title of series, numbering

URL för elektronisk version

<http://urn.kb.se/resolve?urn=urn:nbn:se:liu:diva-20818>

Titel

Title

Combining Reflectometry, Ablation and Fluid Collection in a Microstructured Fiber

Författare

Author

Azizahalhakim Sudirman

Sammanfattning

Abstract

The purpose of the diploma work is to investigate the possibilities to combine three different areas; reflectometry, microfluidics and laser ablation in a microstructured single-mode fiber, thus obtaining a controlled technique for positioning for ablation and collection of liquids from small inclusions.

Each of the three areas is thoroughly described in different sections of this report. The first part of the experiments in this diploma work consisted of combining reflectometry and microfluidics, the second part combining reflectometry with laser ablation and the final experiment setup consisted of a combination of all three areas. An artificial system for liquid collection was then designed for that purpose.

The results obtained from experiments and measurements clearly demonstrate that combining reflectometry, laser ablation and fluid collection in a single optical fiber is promising. Future work will include improvements of the technique towards a medical application for bone marrow transplantation.

Nyckelord

Keyword

reflectometry, microfluidics, laser ablation, microstructured fiber

Abstract

The purpose of the diploma work is to investigate the possibilities to combine three different areas; reflectometry, microfluidics and laser ablation in a microstructured single-mode fiber, thus obtaining a controlled technique for positioning for ablation and collection of liquids from small inclusions.

Each of the three areas is thoroughly described in different sections of this report. The first part of the experiments in this diploma work consisted of combining reflectometry and microfluidics, the second part combining reflectometry with laser ablation and the final experiment setup consisted of a combination of all three areas. An artificial system for liquid collection was then designed for that purpose.

The results obtained from experiments and measurements clearly demonstrate that combining reflectometry, laser ablation and fluid collection in a single optical fiber is promising. Future work will include improvements of the technique towards a medical application for bone marrow transplantation.

Sammanfattning

Syftet med examensarbetet är att studera möjligheterna att kombinera tre olika områden; reflektometri, mikrofluidik och laserablation i en mikrostrukturerad singelmod fiber, för att härigenom utveckla en kontrollerad teknik för positionering av ablation och uppsamling av vätskor i små inklusioner.

De tre olika områdena är beskrivna i detalj i respektive kapitel av rapporten. Första delmomentet i de experiment utförda för examensarbetet bestod av att kombinera reflektometri och mikrofluidik, andra delmomentet var att kombinera reflektometri och laserablation och det slutliga experimentet bestod av en kombination av alla tre områden. Ett artificiellt system för uppsamling av vätskor konstruerades för det syftet.

De resultat erhållna från experiment och mätningar visade tydligt att kombinerad av reflektometri, laserablation och vätskeuppsamling i en enda optisk fiber är lovande. Framtida studier kommer dels att omfatta en förbättring av tekniken i riktning mot en tillämpning inom medicin för benmärgstransplantation.

Acknowledgements

First and foremost I would like to give my thanks and appreciation to my brilliant supervisor, mentor and dear friend, Walter Margulis at Acreo, for whom I have so much respect and admiration. Without his help, enthusiasm and encouragement I could not have completed this work. He has taught me the meaning of courage and has inspired me to always do my best. Thank you for believing me and seeing my potential.

I would also like to show my appreciation to my examiner at Linköping University, Hans Arwin for all of his support. I would like to thank the entire Fiber Photonics department at Acreo for their encouragement and support, to Björn, Carola, Erik, Micke, Patrik, Pierre-Yves, Pär, Ralf and Sasha, and also to the rest of the staff for making me feel so welcome and at home at Acreo.

Last but not least, I would like to thank my wonderful parents for believing in me and encouraging me to accomplish greatness and not settle for anything but the best. I would also like to show my appreciation to Karima, who is my very best friend and is like a sister to me. I thank her for always being there for me with love and support. She truly is my inspiration and I'm so grateful to have her in my life. And I would like to give a big thanks to my amazing friends, both in Stockholm and Linköping, for all the enthusiasm and inspiration you all have given me throughout the years.

Contents

Abstract	vi
Sammanfattning	vi
Acknowledgements	vii
1 Introduction	1
1.1 Background	1
1.2 Objective	1
1.3 Outline	2
2 Optical fibers	3
2.1 Optical fibers	3
2.2 Propagation in optical in fibers	4
2.2.1 Introduction to ray optics	4
2.2.2 Wave representation	6
2.2.3 Modes	6
2.3 Optical properties of fibers	8
2.3.1 Dispersion	8
2.3.2 Fiber attenuation	9
2.4 Polarization behavior in optical fibers	10
2.4.1 Fresnel equations	10
2.5 Optical fiber types and their properties	12
2.5.1 Single-mode fibers	12
2.5.2 Multi-mode fibers	12
3 Optical Low Coherence Reflectometry	13
3.1 Introduction to Optical Low Coherence Reflectometry	13
3.2 High-resolution reflectometer	14
3.2.1 Measuring distances in known materials with a reflectometer	14
3.2.2 Measuring reflection from index change with a reflectometer	15
3.3 Setup for measurements with reflectometer	15
3.4 Measurements on fiber capillaries	16
3.4.1 Results	17
3.5 Measurements on inclusions in glass	17
3.5.1 Results	18
4 Microfluidics and fluid collection	20
4.1 Introduction to microfluidics	20

4.1.1	Surface tension and contact angles	20
4.1.2	Wetting.....	20
4.1.3	Capillary effect.....	21
4.2	Preliminary microfluidics studies	22
4.2.1	Setup	22
4.2.2	Results.....	23
4.3	Microstructured fibers.....	23
4.4	Four ways of allowing for flow	24
4.4.1	Polishing	24
4.4.2	Fiber arrangement with capillary	25
4.4.3	Microexplosion	25
4.4.4	Optical fiber arrangement with an etched STF	26
4.5	Final fiber arrangement.....	26
4.6	Combining reflectometry with fluid collection.....	27
4.6.1	Setup	27
4.6.2	Results.....	30
5	Laser ablation.....	31
5.1	Introduction to laser ablation	31
5.1.1	Nd:YAG Laser	31
5.2	Ablation of sample	32
5.2.1	Preliminary ablation study	32
5.2.2	Results.....	32
5.3	Ablation with an optical fiber combined with reflectometry.....	33
5.3.1	Setup part I.....	33
5.3.2	Setup part II.....	34
5.3.3	Results.....	36
6	Combining reflectometry, ablation and fluid collection.....	37
6.1	Setup	37
6.2	Results.....	39
7	Conclusions and suggestions on future work.....	40
7.1	Conclusions.....	40
7.1.1	Reflectometry and fluid collection.....	40
7.1.2	Reflectometry and laser ablation	40
7.1.3	Final combination	40

7.2	Further improvements on combining ablation and reflectometry.....	40
7.2.1	Use of coupler	41
7.2.2	Use of dichroic filter	41
7.3	More efficient fluid collection	41
8	References.....	43
	Other literature	43

1 Introduction

1.1 Background

A technique using a single optical fiber for positioning, based on low-coherence reflectometry, combined with laser ablation and fluid collection from small inclusions is presently nonexistent. Such a technique could, from a geological point of view, be of huge interest for studying small inclusions in rocks and minerals containing liquids, gases and oils, which have been trapped during the formation of the rocks and minerals, possibly for many millions of years.

If the content of those inclusions could be collected in a controlled way with the help of a measuring technique for positioning, laser ablation could be applied to remove a small amount of the rock or mineral in order to collect a sample from the inclusion with a special microstructured optical fiber designed for that purpose. The fluid sucked into the fiber can then be analyzed with minimal contamination. The same combination technique for positioning, ablation and fluid collection could also be applied in medicine for bone marrow transplantation in order to carve through bone with the ablation technique, and collecting a sample of bone marrow in the microstructured fiber, while observing the positioning with the reflectometer.

1.2 Objective

The present diploma work is part of a long term ambition to contribute to the treatment and diagnostics of leukemia and bone-marrow transplantation. The diploma work is also part of a project aiming to study inclusions in various types of rocks and hopefully even in meteors, for instance from Mars. If a good characterization technique were available for the study of the fluid inclusions avoiding contamination, one could hope to detect signs of life. It could complement the techniques presently employed.

The aim of this diploma work is to combine three different areas; laser ablation, microfluidics and low-coherence reflectometry, thus creating a technique for ablation using a high power laser through an optical fiber with as little damage of the ablated material as possible and for fluid collection from artificial systems into a microstructured fiber, while monitoring both processes with low-coherence reflectometry. It is thus important to have an optical fiber arrangement, which allows light and fluid to be conveyed independently to the region of interest.

The first step of the diploma work is to study low-coherence reflectometry as a tool to characterize small inclusions in glass materials with an optical fiber as probe. The main purpose of low-coherence reflectometry is to not only characterize the depths of inclusions but also to monitor the collection of liquid and the laser ablation process. The next step is to combine fluid collection with the low-coherence reflectometry measuring technique, then to combine low-coherence reflectometry and laser ablation and the final step is to combine all three areas.

1.3 Outline

An introduction to optical fibers and a general description of the optical properties in fibers are given in the following section. The principal of low-coherence reflectometry, along with experiments done with reflectometry and corresponding results are explained in section 3. In section 4, an introduction is given to microfluidics and fluid collection in a fiber. Also different microstructured fiber arrangements are discussed in section 4, with subsections describing methods on how to prepare the microstructured fiber arrangements used in this work and the combination of fluid collection and low-coherence reflectometry. Laser ablation is first introduced in section 5, along with a description of the experiments made with optical fibers and low-coherence reflectometry. The combination of the three areas and experiments done with the setup, along with the results obtained are described in section 6. Conclusions and suggestions for improvements of the technique for future work are given in section 7.

2 Optical fibers

2.1 Optical fibers

An optical fiber is a string composed of dielectric materials, which can guide optical radiation. [1] The optical fiber consists of two materials, one is called the cladding surrounding the inner material defined as the core of the fiber, as illustrated in Fig. 1. The fiber core carries, due to reflection at the boundary between the two dielectric materials, most of the transmitted light through the optical fiber. Various glasses of silica are commonly used for manufacturing the fiber core and cladding. Plastic coatings are added to optical fibers for mechanical protection in normal environments.

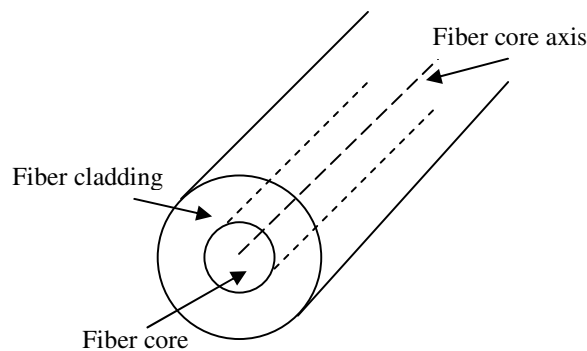


Figure 1: Illustration of an optical fiber, with its core and cladding.

This section introduces the fundamentals of optical properties in fibers. The simplest way to understand optical properties is to investigate the behavior of light at the boundary between the fiber core and cladding which have differing refractive indices. The refractive index of a material, n , is the ratio of speed of light in vacuum, c , to its speed in the material, v , given in equation (2.1). Accordingly, light propagates more slowly in materials with a high refractive index than in materials with a lower refractive index.

$$n = \frac{c}{v} \quad (2.1)$$

To use optical fibers in practice, one must be able to produce smooth and clean endfaces in order to trap light at one end of the fiber and guide the light through the fiber. [1] It may be necessary to connect optical fibers together using permanent joints. A permanent joint is normally termed a 'splice', and is formed often by fusion methods. The fibers are heated to their melting point by an electric arc and are brought into contact to produce a seamless joint. Good quality endfaces are required, to be prepared initially, when splicing optical fibers.

2.2 Propagation in optical fibers

The concept of fiber propagation is basically the theory of light transmission through an optical fiber. [1] In this section the guidance of light and the approximation of light through an optical fiber are discussed. The behavior of light within the optical fiber is described with the theory of wave representation, and is suitable when speaking of optical properties such as fiber absorption, dispersion and attenuation.

2.2.1 Introduction to ray optics

The direction of a ray of light travelling from a material with a higher refractive index to a material with a lower refractive index, $n_1 > n_2$, is governed by Snell's law of refraction. The direction of the transmitted beam is then given by

$$n_1 \sin \theta_i = n_2 \sin \theta_t \quad (2.2)$$

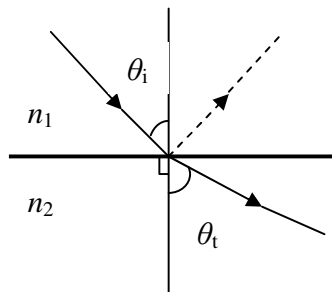


Figure 2: Refraction at a dielectric interface when the angle of incidence is less than the critical angle.

where θ_i is the angle of incidence and θ_t is the angle of refraction. As θ_i increases to a point where $\theta_t = 90^\circ$, as illustrated in Fig.3a, the specific value of θ_i is then termed the critical angle of incidence, θ_c . The critical angle is according to Snell's law described by equation (2.3). A further increase of θ_i results in that the incident light beam becomes totally reflected at the boundary, as illustrated in Fig. 3b.

$$\theta_c = \sin^{-1}\left(\frac{n_2}{n_1}\right) \quad (2.3)$$

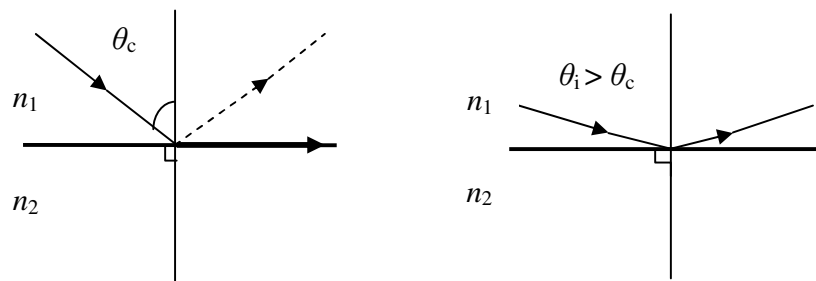


Figure 3: (a) An incoming light beam at the critical angle results in a refraction angle equal to 90° . (b) Total reflection of the light beam occurs when the angle of incidence is larger than the critical angle.

Three factors affect the light collecting ability of an optical fiber. [1] First is the physical size of the fiber core, the second is the maximum angle between the direction of the incoming light and the fiber core axis, defined as the acceptance angle θ_0 , and the third is the shape of the refractive index distribution within the core of the fiber. The maximum acceptance angle is limited by the critical angle of the light incidence at the core-cladding boundary.

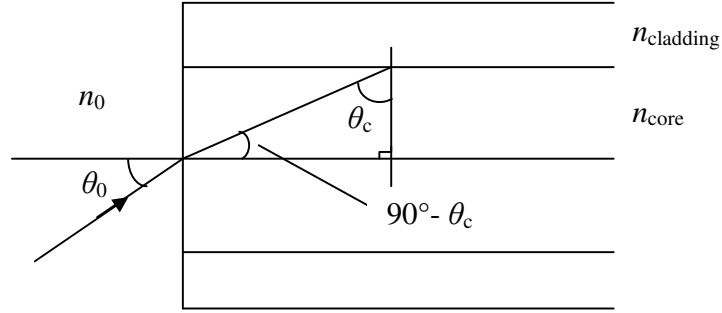


Figure 4: Maximum acceptance angle of an optical guide.

Fig. 4 illustrates a travelling ray of light in a medium of refractive index n_0 entering the front face of an optical fiber, with refractive index n_{core} , at an angle θ_0 to the fiber axis core subsequently striking the core-cladding boundary at the critical angle θ_c . Take into account that in Fig. 4 $n_0 < n_{core}$ and $n_{core} > n_{cladding}$. From Snell's law the following is then given

$$n_0 \sin \theta_0 = n_{core} \cos \theta_c \quad (2.4)$$

The acceptance angle is determined by the refractive indices of the core, the cladding and the surrounding medium of the fiber and is related to the numerical aperture of the optical fiber. The numerical aperture is a dimensionless number, which characterizes the range of angles which the optical fiber can emit and trap light and is defined as $n_0 \sin \theta_0$. [2] The numerical aperture can be rewritten with the help of equation (2.3) and (2.4) and is then expressed as

$$NA = n_0 \sin \theta_0 = n_{core} \sqrt{1 - \sin^2 \theta_c} = \sqrt{n_{core}^2 - n_{cladding}^2} \quad (2.5)$$

Two types of rays can propagate along an optical fiber. [3] The first type is called meridional rays, which are rays that pass through the axis of the optical fiber and can be classified as bound or unbound rays. Bound rays remain in the fiber core and propagate along the axis of the fiber. The second type of rays is termed skew rays, which are rays that travel through an optical fiber without passing through its axis.

2.2.2 Wave representation

Electromagnetic wave theory is used to describe light propagation in an optical fiber. [4] Light is then described as waves, not rays. The wave representation suggests that a light wave can be represented as plane waves. A plane wave is a wave whose surfaces of constant phase are infinite parallel planes normal to the direction of propagation, and is described by its direction, amplitude, and wavelength of propagation. [5] A plane wave propagating in the z -direction can be described in the following form

$$u(z, t) = Ae^{j(kz - \omega t)} \quad (2.6)$$

where j is the imaginary unit, \mathbf{k} is the wave vector, ω is the angular frequency, and A is the amplitude. The wave planes having the same phase are called wavefronts, and are required to remain in phase in order for light to be guided through the optical fiber. Only those wavefronts with an incidence on the optical fiber corresponding to internal angles equal or less to the critical angle can propagate within the fiber. If propagating wavefronts are not in phase they disappear, due to destructive interference. The interference which occurs is the reason why only a limited number of modes can propagate within the optical fiber.

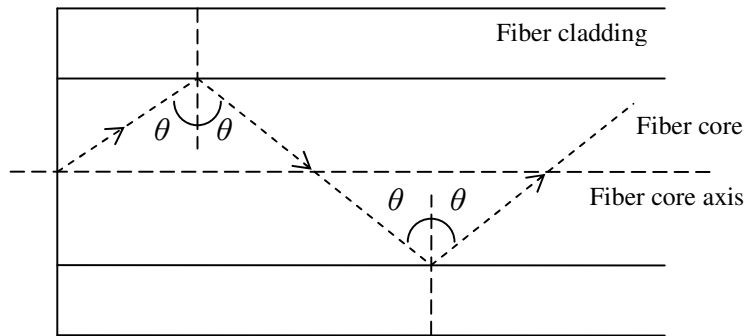


Fig.5: Illustration of light propagating within an optical fiber.

The propagation constant of an electromagnetic wave is a measure of the change undergone by the amplitude of the wave as it propagates in a given direction. The propagation constant, β , along the fiber axis is described in equation (2.7), where λ is the wavelength of the light propagating and the angle θ is illustrated in Fig. 5.

$$\beta = \frac{2\pi n_{core} \sin \theta}{\lambda} \quad (2.7)$$

2.2.3 Modes

Maxwell's equations describe electromagnetic waves, the modes of an optical fiber, as having two components, the electric field, $E(x, y, z)$, and the magnetic field, $H(x, y, z)$. [4] The direction of the electric field, E , is perpendicular to the direction of the magnetic field, H . Modes propagating along the axis of the optical fiber are said to be transverse. When the electric field is perpendicular to the direction of propagation and the magnetic field, the transverse modes are said to be TE modes. Another type of transverse modes

are the TM modes, the magnetic field is then perpendicular to both the direction of propagation and the electric field.

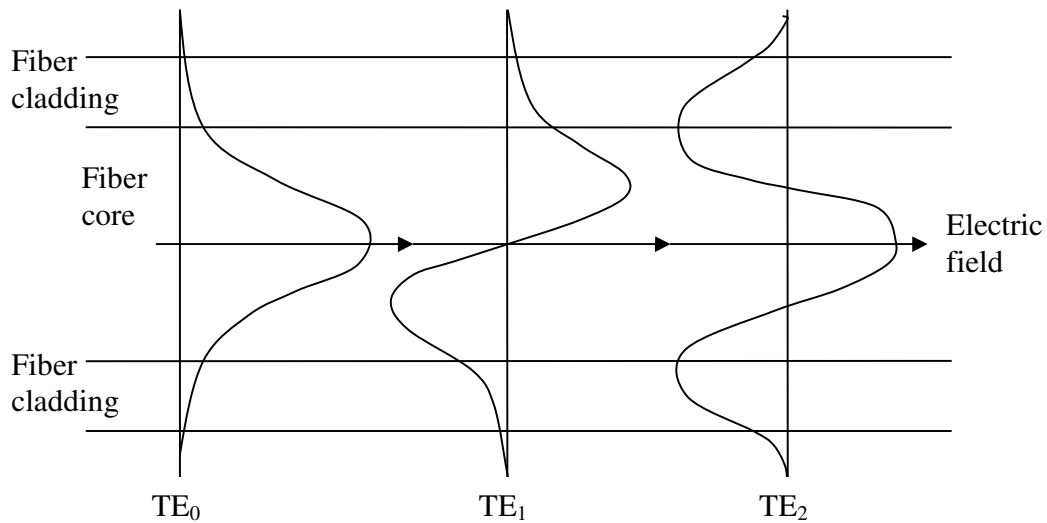


Figure 6: Transverse electric (TE) mode field patterns.

The TE mode field patterns, illustrated in Fig. 6, are indicated by the number of field maxima within the fiber core the order of each mode. As seen in Fig. 6, TE_0 has one field maxima and TE_1 has two etc. TE_0 is considered to be the fundamental mode, where the electric field is at maximum at the center of the fiber core axis and decays toward the boundary of the fiber core-cladding. If the magnetic fields are also taken into consideration when describing mode field patterns, the transverse electromagnetic field distribution is then called TEM_{mn} . The index numbers m and n indicate the modes in the x and y direction. The intensity distribution of various modes, where TEM_{00} is the fundamental mode, is given in Fig. 7.

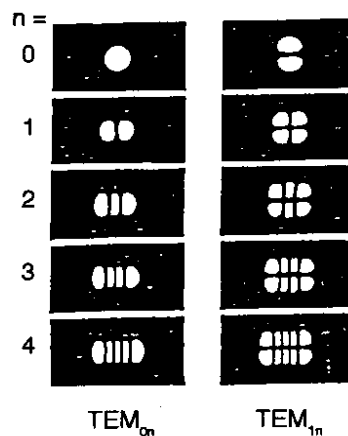


Figure 7: Transverse electromagnetic field distributions of modes for $m=0$ and $m=1$. Source: Dirk B, (1991).

As the number of field maxima increases, the order of the mode also increases. [4] If the number of field maxima is higher than five the transverse modes are called high-order

modes. Part of the modes then extends into the cladding. Low-order modes penetrate the cladding only to some extent, due to the fact that the electromagnetic fields are concentrated in the fiber core region. In high-order modes the electromagnetic fields are distributed more toward the outer edges of the fiber.

As the modes propagate within the fiber, mode coupling occurs, which is the exchange of power between the fiber core modes and the cladding modes and result in a loss of power from the core modes. [4] In addition, there are also leaky modes which lose power as they propagate within the optical fiber. For a mode to remain within the core of the fiber, the propagation constant, β , of a mode must meet certain boundary conditions given in (2.8). If the propagation constant is smaller than $2\pi n_{\text{cladding}}/\lambda$, power then leaks out of the fiber core and into the fiber cladding.

$$\frac{2\pi n_{\text{cladding}}}{\lambda} < \beta < \frac{2\pi n_{\text{core}}}{\lambda} \quad (2.8)$$

For a given mode, a change in wavelength can prevent the mode from propagating along the optical fiber. [1] The mode is then said to be cut off. An optical fiber is always able to propagate at least one mode, the fundamental mode of the fiber, which never can be cut off. The wavelength preventing the next higher mode from propagating is called the cutoff wavelength. The normalized frequency, a dimensionless quantity, determines how many modes an optical fiber can support and is related to the cutoff wavelength of the fiber. The normalized frequency is defined in equation (2.9), where d is the fiber core diameter and λ is the wavelength of light in air. The number of modes supported by the optical fiber is increased, when the normalized frequency increases. [4]

$$V = \frac{2\pi d}{\lambda} \sqrt{n_{\text{core}}^2 - n_{\text{cladding}}^2} = \frac{2\pi d}{\lambda} NA \quad (2.9)$$

2.3 Optical properties of fibers

2.3.1 Dispersion

The information-carrying capacity of an optical fiber is limited by dispersion, due to the introduction of small time changes for signals propagating within the fiber. [1] It is worth mentioning that energy and information travel not at the phase velocity v_p , see equation (2.10), but at the velocity known as the group velocity, v_g , which can differ from the phase velocity of a wave. The phase velocity is given by the frequency of the wave divided by its propagation constant. The group velocity, however, is given by equation (2.11), where ω is the angular frequency and k is the wave number.

$$v_p = \frac{\omega}{\beta} \quad (2.10)$$

$$v_g = \frac{d\omega}{dk} \quad (2.11)$$

Dispersion in an optical fiber occurs due to changes in the propagation constant. [6] The change in the propagation constant for different wavelengths is called chromatic dispersion, and can occur in all types of optical fibers. Chromatic dispersion depends on optical fiber materials and occurs because light with different wavelengths propagate through materials and waveguides at different speed. There are two types of chromatic dispersion, material dispersion and waveguide dispersion. Material dispersion occurs because the distribution of light is dependent on the relationship between the wavelength and refractive index of the fiber core. Different wavelengths travel at different speeds in the optical fiber material. Thus, light that enters a fiber at one time can exit the fiber at different times depending on wavelength. Waveguide dispersion occurs due to the fact that light propagates differently in the fiber core than in the fiber cladding. The change in propagation constant for different modes is called modal dispersion, and causes the input light to spread. As the modes propagate within the optical fiber, light energy distributed among the modes is delayed by different amounts. The light spreads because each mode propagates along the fiber at different speeds. Since modes travel in different directions, some modes travel longer distances. As the length of the fiber increases the modal dispersion increases.

2.3.2 Fiber attenuation

Attenuation reduces the amount of optical power transmitted by a fiber. [16] Attenuation determines the distance an optical signal can travel and is mainly a result of light absorption, scattering, and bending losses. There are two categories of fiber attenuation. The first includes all of intrinsic sources of loss arising from the design and the material of the fiber. The second category contains sources extrinsic to the fiber, arising from the deployment and environmental factors. Attenuation is described as the ratio of optical input power, P_i , to the optical output power, P_o . Equation (2.12) defines attenuation as a unit of length, where the length, L , is expressed in kilometers. Hence the unit for signal attenuation is dB/km.

$$attenuation = \left(\frac{10}{L} \right) \log_{10} \left(\frac{P_i}{P_o} \right) \quad (2.12)$$

Each mechanism of loss is influenced by the properties and structure of the optical fiber. [7] Loss can also be present at fiber connections. Absorption is defined as the amount of attenuation resulting from the conversion of optical power into another energy form, such as heat. Absorption in optical fibers is explained by the intrinsic/extrinsic properties and the imperfections in the atomic structure of the fiber material. Absorption occurs when a photon interacts with an electron and excites it to a higher energy level. In fiber optics, silica fibers are often used because of their low intrinsic material absorption at the wavelengths of operation. In silica glass, the wavelengths of operation range from 700 nm to 1600 nm. In silica glass, absorption is caused by the vibration of silicon-oxygen (Si-O) bonds. The interaction between the vibrating bond and the electromagnetic field of the optical signal causes intrinsic absorption. Light energy is transferred from the electromagnetic field to the bond. Extrinsic absorption is caused by i.e. metal impurities in the optical fiber material introduced during manufacturing. Extrinsic absorption is

caused by the transition of these metal ions from one energy level to another. Extrinsic absorption also occurs when hydroxyl ions (OH⁻) are introduced into the optical fiber.

Scattering losses are caused by the interaction of light with density changes within an optical fiber. During manufacturing, regions of higher and lower molecular density areas (relative to the average density of the fiber) are created thus resulting to density changes within the fiber. Light is then partially scattered in all directions. In commercial optical fibers the main source of loss is called Rayleigh scattering, which occurs when the size of the fiber defect is less than one-tenth of the operating wavelength of light. As the wavelength increases the loss caused by Rayleigh scattering decreases. If the size of the defect is greater than one-tenth of the wavelength of light the scattering is called Mie scattering, which scatters light out of the fiber core. However, in commercial optical fibers the effects of Mie scattering are insignificant, due to the fact that optical fibers are manufactured with very few large defects.

Bending a fiber also causes attenuation. Loss from bending is classified according to the bend radius of curvature, as either microbend loss or macrobend loss. Macrobends are bends with a large radius of curvature relative to the fiber diameter. If optical fibers are bent too sharply, macrobend losses occur. Microbends are small microscopic bends of the fiber core axis that occur mainly when a fiber is cabled, but loss can still occur even if the optical fiber is cabled correctly. Microbend losses are caused by small discontinuities or imperfections in the fiber. Uneven coating applications and improper cabling procedures increase microbend loss. Microbends change the path of the propagating modes. Light propagating at the inner side of the bend travels a shorter distance than that on the outer side. To maintain the phase of the light wave, the mode phase velocity must increase.

2.4 Polarization behavior in optical fibers

For transverse waves, polarization describes the orientation of the oscillations of the electric field in the plane perpendicular to the wave's direction of propagation. [8] The oscillations may be oriented in a single direction then called linear polarization or the oscillation direction may rotate as the wave propagates also known as circular or elliptical polarization. Circularly polarized waves can rotate rightward or leftward in the direction of propagation. Which of those two rotations is present in a wave is called the chirality of the wave.

2.4.1 Fresnel equations

Fig. 8 illustrates a light wave incident on a surface described by electric fields polarized in the plane of incidence (\parallel) and perpendicular to the plane of incidence (\perp). Also shown are the reflected and refracted light wave directions with respective polarized electric fields. This illustration with polarized electric fields is helpful when the Fresnel equations are to be described. Note that the relation between refractive indices is $n_1 > n_2$ in Fig. 8.

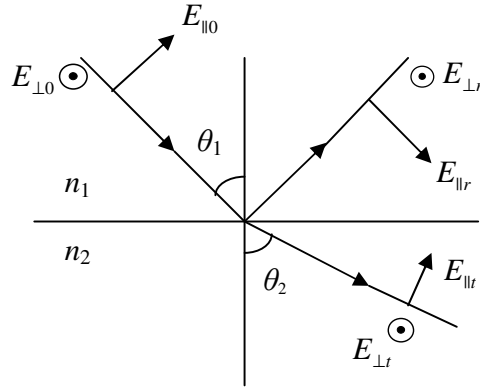


Figure 8: Illustration of incoming reflected and refracted light with polarized electric fields. Source: *Physics Handbook, (1999)*.

The fraction of the incident power reflected from the interface between the two media with indices n_1 respective n_2 is given by the reflectance R , and the fraction of incident power refracted is given by the transmittance T . [9] Note also that the media are assumed to be non-magnetic. The calculations of R and T depend on polarization of the incident light. If the incident light is polarized with the electric field parallel to the plane of incidence R is given by equation (2.13) and if the light is polarized with the electric field perpendicular to the plane of incidence the reflection coefficient is given by equation (2.14)

$$R_{\parallel} = \left(\frac{\tan(\theta_i - \theta_t)}{\tan(\theta_i + \theta_t)} \right)^2 = \left(\frac{n_1 \cos \theta_i - n_2 \cos \theta_t}{n_1 \cos \theta_i + n_2 \cos \theta_t} \right)^2 \quad (2.13)$$

$$R_{\perp} = \left(\frac{\sin(\theta_i - \theta_t)}{\sin(\theta_i + \theta_t)} \right)^2 = \left(\frac{n_1 \cos \theta_t - n_2 \cos \theta_i}{n_1 \cos \theta_i + n_2 \cos \theta_t} \right)^2 \quad (2.14)$$

The transmission coefficient of the polarized light parallel to the plane of incidence and the corresponding transmission coefficient of the polarized light perpendicular to the plane of incidence are described in equations (2.15) respective (2.16)

$$T_{\parallel} = \left(\frac{2 \cos \theta_i \sin \theta_t}{\sin(\theta_i + \theta_t) \cos(\theta_i - \theta_t)} \right)^2 = \left(\frac{2n_1 \cos \theta_i}{n_1 \cos \theta_i + n_2 \cos \theta_t} \right)^2 \quad (2.15)$$

$$T_{\perp} = \left(\frac{2 \cos \theta_i \sin \theta_t}{\sin(\theta_i + \theta_t)} \right)^2 = \left(\frac{2n_1 \cos \theta_t}{n_1 \cos \theta_i + n_2 \cos \theta_t} \right)^2 \quad (2.16)$$

If the light is at near-normal incidence to the interface, meaning that $\theta_i \approx \theta_t \approx 0$, the reflectance and transmittance simplifies to equations (2.17) and (2.18), respectively. Equations (2.13-2.18) are known as the Fresnel equations, and are essential for the understanding of the behavior of light waves within the optical fiber.

$$R = R_{\parallel} = R_{\perp} = \left(\frac{n_1 - n_2}{n_1 + n_2} \right) \quad (2.17)$$

$$T = T_{\parallel} = T_{\perp} = \frac{4n_1n_2}{(n_1 + n_2)^2} \quad (2.18)$$

2.5 Optical fiber types and their properties

Optical fibers are characterized by their structure and by their properties of light transmission. [10] Optical fibers are classified into two types, single-mode and multi-mode fibers, and are classified by the number of modes that propagate within the fiber. The structure of the optical fiber can either permit or restrict modes from propagating within the fiber.

2.5.1 Single-mode fibers

The physical difference between an optical single-mode fiber and an optical multi-mode fiber is the size of the fiber core. The core diameter of a single-mode fiber is about 8-10 μm and the outer diameter is often 125 μm . The single-mode fiber is designed to guide only a single mode of light, the fundamental mode, which can contain a variety of wavelengths. Single-mode fibers used in telecommunications operate at 1310 or 1550 nm and require expensive laser sources. Optical single-mode fibers exist for nearly all visible wavelengths of light. Single-mode fibers are manufactured with the same materials and the same fabrication process as multi-mode fibers. [1] Material and waveguide dispersion are more or less related in single-mode fibers. Modal dispersion does not exist in single-mode fibers. Single-mode fibers exhibit the highest possible bandwidth.

2.5.2 Multi-mode fibers

Multi-mode fibers can propagate over 100 modes. [11] The number of modes allowed to propagate depends on the size of the fiber core and the numerical aperture of the fiber. As the fiber core size and numerical aperture increase, the number of modes increases. Typical values of multi-mode fiber core size are 50-100 μm . A large core size and a high numerical aperture lead to easier light trapping in the fiber and also easier production of fiber connections. Another advantage is that multi-mode fibers allow the use of light-emitting diodes (LEDs), operating at a wavelength of 850 nm. LEDs are preferred in some applications because they are cheaper, less complex, and last longer than laser sources. Fiber manufacturers adjust the fiber core diameter, numerical aperture and index profile properties of multi-mode fibers to maximize the bandwidth. In multi-mode fibers, waveguide dispersion and material dispersion are separate properties. Waveguide dispersion is small, compared to material dispersion, and is usually neglected. Modal dispersion is the dominant source of dispersion in multi-mode fibers.

3 Optical Low Coherence Reflectometry

3.1 Introduction to Optical Low Coherence Reflectometry

Optical Low Coherence Reflectometry (OLCR) is a coherent detection technique based on Michelson interferometry, also known as white-light interferometry [12]. A simple schematically illustration of OLCR is given in Fig. 9. A continuous working low-coherence light source is coupled to a fiber optic coupler, which splits the low-coherent signal into a reference arm and a signal arm. The optical delay for the reflected light in the reference arm is varied by translating the movable mirror. If the optical delay of the reflected light from the reference arm matches the delay from the returning light in the signal arm, interference occurs. The interference only occurs if the optical distance to the reference mirror is within a coherence length compared to the optical distance of the signal arm. If the distance is more than a coherence length only continuous working power is registered, since the reflected signals do not interfere. The interference signal reaches a detector and strips away the unwanted interference fringes. The signal then becomes proportional to the square root of the optical reflectivity. The output signal is squared and displayed as a function of mirror position, in order to obtain a reflectivity trace seen in Fig. 9.

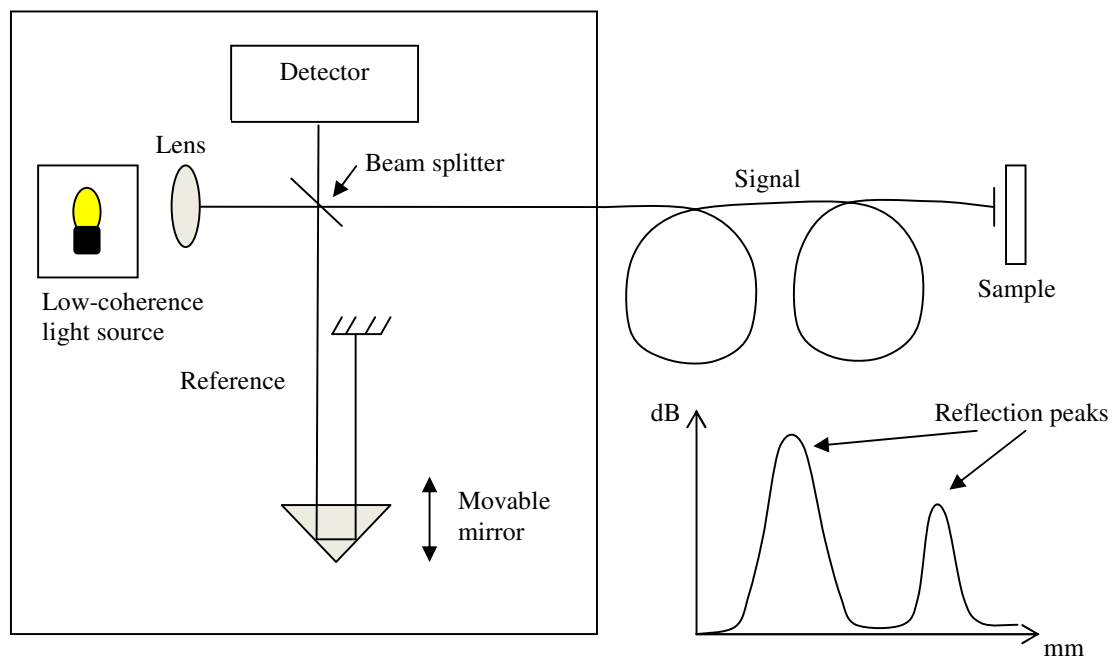


Figure 9: A simple schematically illustration of OLCR.

3.2 High-resolution reflectometer

The Ando model AQ7410B Reflectometer used for this diploma work is based on low-coherence reflectometry. The reflectometer consists of two parts (see Fig. 10), one part where the measurements take place with the movable mirrors, and the other part where the signal is being processed in order to obtain and display the reflectivity trace. The operating wavelength of the low-coherent continuous working light source can be set to either 1550 nm or 1310 nm. The spatial resolution is $\sim 20 \mu\text{m}$ and the measurement range is 2000 mm. The refractive index is set to 1.462, meaning that the reflectometer measures the reflectivity in different media with the refractive index of glass. The two axes display the absolute position of the reflections in millimeters and the reflectivity is measured in decibels (dB). The reflectometer can also be connected to a computer, as seen in Fig. 10, in order to store measured data.



Figure 10: An image of the Ando AQ7410B Reflectometer

3.2.1 Measuring distances in known materials with a reflectometer

When measuring the distance between the absolute positions of reflection peaks one must always take into account that light travels faster in media with a lower refractive index than in a medium with a higher index of refraction, as mentioned in the previous section. From Snell's law equation (3.3) is given, obtaining an equation only dependent on the refractive indices of each media and speed of light in both media.

$$\frac{\sin \theta_1}{\sin \theta_2} = \frac{n_2}{n_1} = \frac{v_1}{v_2} \quad (3.3)$$

Further, the speed of light in a medium, v , can be rewritten as the ratio of distance, d , to time, t . The assumption t_{medium} equal to $t_{\text{reflectometer}}$ is made here, hence resulting in

$$d_{\text{medium}} n_{\text{medium}} = d_{\text{reflectometer}} n_{\text{reflectometer}} \quad (3.4)$$

The refractive index of the medium is mostly known and the refractive index of the reflectometer is set to 1.462. From measurements with the reflectometer the distance between absolute positions of reflection peaks is obtained. Hence the distance in the medium can be calculated as following

$$d_{\text{medium}} = \frac{1.462 \cdot d_{\text{reflectometer}}}{n_{\text{medium}}} \quad (3.5)$$

3.2.2 Measuring reflection from index change with a reflectometer

The reflectance, R , for water-air, glass-air and glass-water are calculated as shown in equations (3.6)-(3.8) with the help of Fresnel equation, when the incident light beam is very near normal. These values can be helpful when estimating the amount of reflected light, due to refractive index change in various media.

$$R_{\text{air} \rightarrow \text{water}} = \left(\frac{n_{\text{air}} - n_{\text{water}}}{n_{\text{air}} + n_{\text{water}}} \right)^2 = R_{\text{water} \rightarrow \text{air}} \approx 2\% \quad (3.6)$$

$$R_{\text{air} \rightarrow \text{glass}} = \left(\frac{n_{\text{air}} - n_{\text{glass}}}{n_{\text{air}} + n_{\text{glass}}} \right)^2 = R_{\text{glass} \rightarrow \text{air}} \approx 4\% \quad (3.7)$$

$$R_{\text{water} \rightarrow \text{glass}} = \left(\frac{n_{\text{water}} - n_{\text{glass}}}{n_{\text{water}} + n_{\text{glass}}} \right)^2 = R_{\text{glass} \rightarrow \text{water}} \approx 0.2\% \quad (3.8)$$

The predicted change (in amplitude) of the reflected light in dB, due to index-matching, is calculated with equation (3.9). Where R_0 is the reflectance and R_1 is the reflectance due to index-matching.

$$\text{Amplitude change} = 10 \log_{10} \left(\frac{R_0}{R_1} \right) \quad (3.9)$$

3.3 Setup for measurements with reflectometer

The aim with the low-coherence reflectometry experiment is to investigate if the depth of inclusions in glassy materials can be measured with the help of a reflectometer. The wavelength of the continuous working low-coherent light source of the reflectometer is set to 1310 nm. The reflectometer has a reference fiber with a length of 213 cm and a

signal fiber that is 200 cm, both 125 μm single-mode fibers with a 10 μm diameter core. The signal fiber is during the measurements coupled to a standard telecom fiber (STF) with a length of 100 cm, and the two will be referred to as the test fiber. The low-coherent signal propagates within the test fiber and passes through two optical lenses in free-space before reaching the sample. The distance between the sample and the first lens is 12.5 cm and the distance between the sample and the second lens is 32 cm. Other resources included in the setup are a microscope and a HeNe laser. The experimental setup is illustrated in Fig. 11.

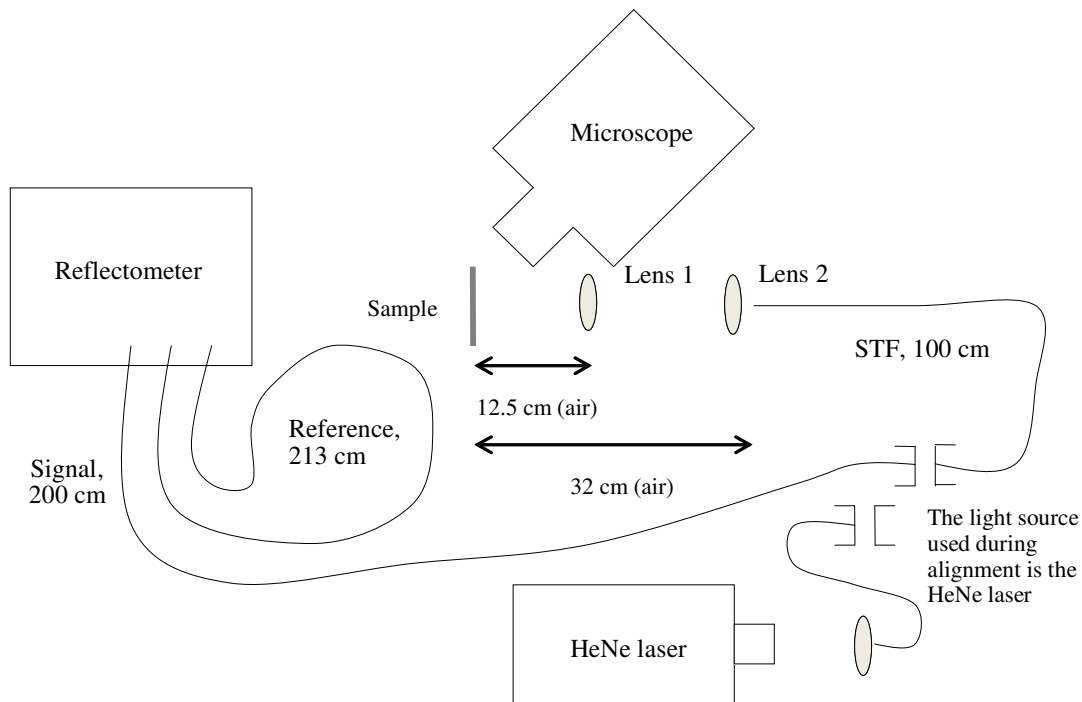


Figure 11: Experimental setup for measurements done with the high-resolution reflectometer.

3.4 Measurements on fiber capillaries

Before measuring inclusions in glass, similar studies are made on fiber capillaries to determine the inner diameter of the capillaries using the same measuring method. Fiber capillaries with known inner diameter of 130 μm (antifiber), 45 μm and 25 μm are used as samples. Fig. 12a illustrates the measurement made on an optical fiber with a 25 μm diameter capillary. The distance between the two outer reflection peaks illustrates the total outer diameter of the capillary, and the distance between the two inner reflection peaks illustrates the inner diameter of the fiber capillary.

Part of the experiment made (on fiber capillaries) is also to investigate the reflection change in amplitude, due to index-matching. Without changing the setup for the experiment, the 25 μm diameter capillary is filled with deionized water. As illustrated in Fig. 12b, the two inner reflections decrease and the distance between them increases, which is the behavior expected.

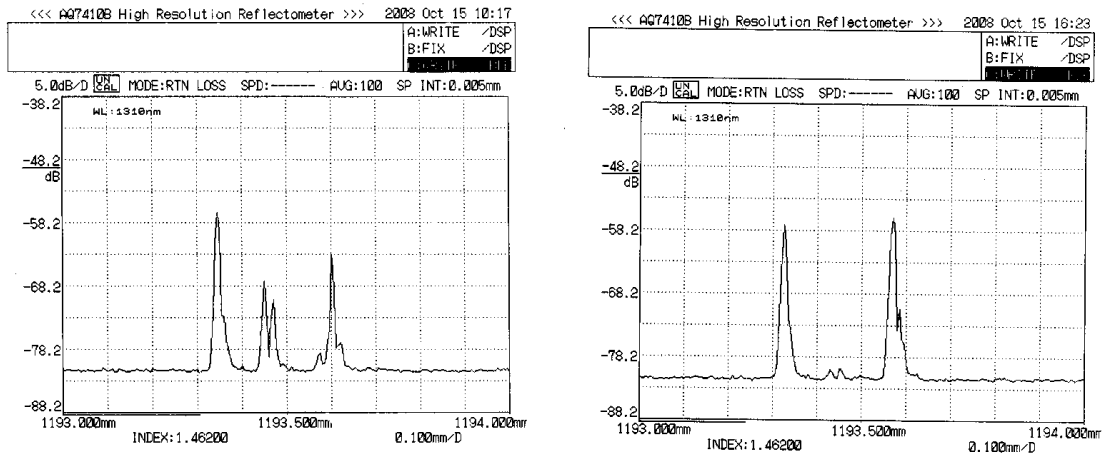


Figure 12: Illustrates the reflectivity obtained from both the capillary's inner and outer diameter (a) without and (b) with index matching.

3.4.1 Results

According to calculations made earlier (see section 3.2.2) on reflectance using Fresnel equations and the formula for amplitude change, the reflectance for air-glass is 4% and for water-glass 0.2%, the amount of light then expected to be reflected due to index-matching is an amplitude change (decrease) of ~13 dB, which is equal to a 20 times decrease of amplitude. Note that the two reflections do not have the same amplitude to start with.

3.5 Measurements on inclusions in glass

For measuring inclusions, a glass sample with a thickness of ~0.5 mm and a diameter of 29 mm is used. The sample front surface is polished before the measurement to increase its transmission. The HeNe laser is used as a light source during the alignment of the setup, and is coupled to the 100 cm single-mode STF. An alignment is necessary for identification and to ensure that an optimal amount of the reflected signal is measured by the reflectometer. The first step of the experiment included selecting a specific inclusion on the glass sample, see Fig. 13c. With the help of the microscope the inclusion to be measured could easily be detected, seen in Fig. 13.a, and illuminated with the HeNe laser, as illustrated in Fig. 13b. Also when aligning, the focus of the light signal passing through the two lenses is adjusted, thus obtaining the largest amount of reflected light from the inclusion.

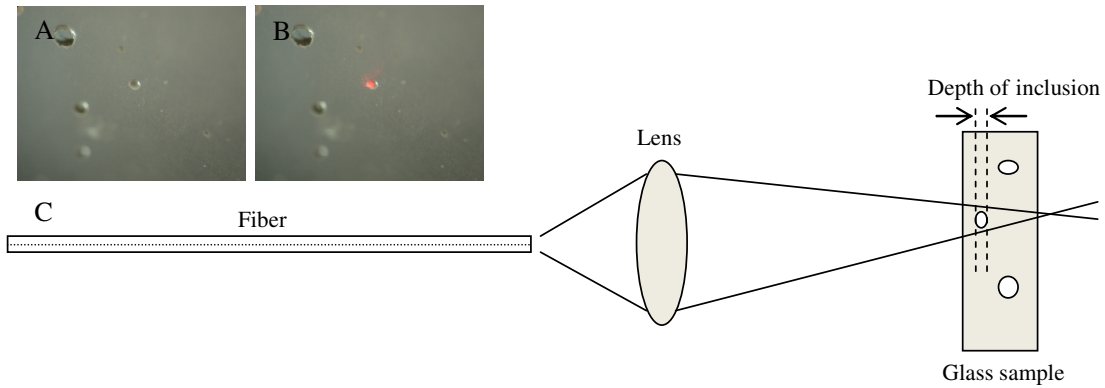


Figure 13: (a) An image of an inclusion in glass taken with the microscope. (b) The (same) inclusion is illuminated with the HeNe laser. (c) Illustration of illuminating an inclusion in a glass sample with a fiber.

After completed alignment, the reflectometer with its signal fiber is coupled to the 100 cm STF for measurements. The low-coherence signal from the reflectometer is guided through the test fiber and illuminates the front and back surfaces of the sample and the inclusion at different distance, resulting in reflections at different absolute positions. The reflection peaks are a result from occurring interference between the optical signals in the test fiber and the reference fiber. The amplitude of the reflection demonstrated the intensity of light reflected back from that particular surface.

3.5.1 Results

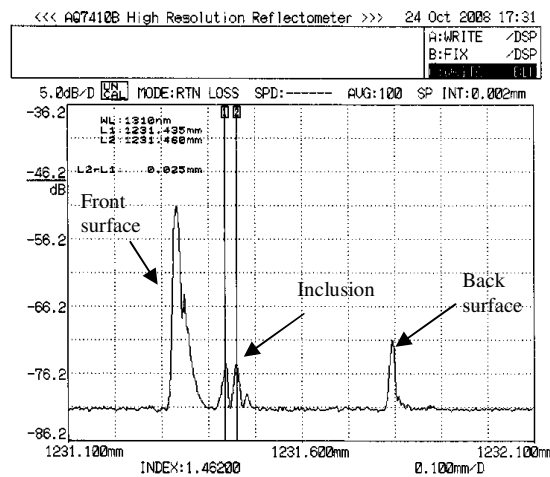


Figure 14: Illustration of a measurement with the reflectometer on an inclusion in glass. The two marked reflection peaks demonstrate the size of the inclusion.

The results of the measurements made with the reflectometer are illustrated in Fig. 14. The most essential information obtained is that the reflection peak to the left with the highest amplitude illustrates the front sample surface and the reflection peak most to the right shows the sample back surface. The measured distance between the two reflections demonstrates the thickness of the sample, which is measured to be ~0.5 mm. The depth of the inclusion (assuming a homogenous inclusion) is given by the absolute position of the

reflections in relation to the sample surfaces. The distance between the two marked reflection peaks in Fig. 14 illustrates the beginning and end points of the inclusion, a distance of 25 μm . Assuming also that the inclusion is air-filled, the refractive index of the inclusion has to be taken in consideration when determining the depth. The distance between the reflections measured is shorter than the actual depth of the inclusion, due to the fact that light travels faster in air than in glass. The size of the inclusion is then calculated to be 37 μm .

4 Microfluidics and fluid collection

4.1 Introduction to microfluidics

Microfluidics studies the behavior of fluids in microscale. Microfluidic behavior can differ from fluid behavior in the macroscale when speaking of factors such as surface tension and fluid flow. The fluid collection part of the diploma work includes microfluidic studies. It is therefore important to understand the microfluidic behavior.

4.1.1 Surface tension and contact angles

Surface tension is caused by various molecular attraction forces between molecules in the liquid. [13] At the surface of the liquid, the molecules are drawn inwards by other molecules deeper inside the liquid and are not attracted as much to molecules in the neighboring medium. A liquid molecule in contact with a neighboring liquid molecule is in a lower state of energy than a molecule not in contact with neighboring molecules. The molecules within the liquid all have as many neighbors as possible, but the liquid molecules at the boundary have fewer neighbors than the molecules deeper inside the liquid, and are therefore in a much higher state of energy. For the liquid to minimize its energy state, it must minimize its number of boundary molecules and must therefore minimize its surface area.

The surface of any liquid is an interface between that liquid and some other medium. Surface tension is not a property of the liquid alone, but a property of the interface of the liquid with some other medium. Where the two surfaces meet their geometry must be such that all forces balance and they form a contact angle, θ_c , which is the angle the tangent to the liquid surface makes with the solid surface. Fig. 15 illustrates the solid-liquid, liquid-vapor and solid-vapor surface tensions.

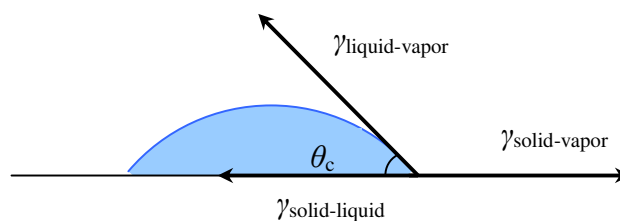


Figure 15: Illustration of a drop of liquid on a solid surface, and the different surface tensions and contact angle

4.1.2 Wetting

Wetting is the ability of a liquid to maintain contact with a solid surface, which is a result from interactions between molecules when the two are brought together. [14] The amount of wetting is determined by a balance of force between adhesive and cohesive forces. Adhesive forces between a liquid and a solid surface cause a liquid drop to spread across the solid surface. Cohesive forces within the liquid cause the drop to minimize its surface area and avoid contact with the solid surface. Wetting and the forces controlling wetting

are also responsible for other related effects, such as the capillary effect. Despite the amount of wetting, the shape of a liquid drop on a solid surface is more or less a truncated sphere. Various amounts of wetting are illustrated in Fig. 16. A drop of liquid tends to spread out over a solid surface as the contact angle decreases. A contact angle less than 90° indicates that wetting of the solid surface is very favorable, resulting in that the liquid spread over a large area of the surface. Contact angles greater than 90° indicate that wetting of the surface is unfavorable, thus resulting in the fluid minimizing its contact with the solid surface.

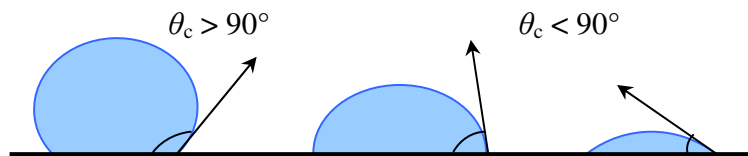


Figure 16: Illustrates drops of liquid with different contact angles.

4.1.3 Capillary effect

If a hollow cylinder has a sufficiently small hole and the liquid adhesion to the walls of the cylinder is sufficiently strong, surface tension can draw the liquid up into the cylinder. [15] This phenomenon is known as the capillary effect. The height the liquid is lifted is given by

$$h = \frac{2\gamma_{\text{liquid-air}} \cos \theta_c}{\rho g r} \quad (4.1)$$

where h is the height the liquid is lifted, $\gamma_{\text{liquid-air}}$ is the liquid-air surface tension, ρ is the density of the liquid, r is the radius of the cylinder, g is the acceleration due to gravity and θ_c is the contact angle. Note that if the contact angle is greater than 90° , the liquid tends to be depressed rather than lifted.

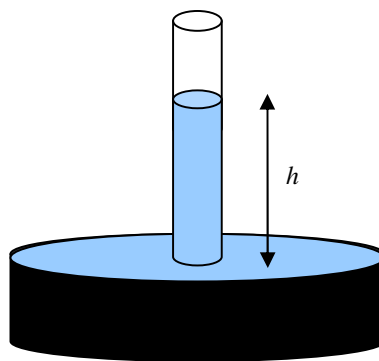


Fig.17: Illustration of the capillary effect

4.2 Preliminary microfluidics studies

A preliminary microfluidics study with the reflectometer is made to investigate the possibility to detect a layer of liquid on a ~ 1 mm thick glass slide using an optical fiber as probe.

4.2.1 Setup

The experimental setup for the preliminary study is illustrated in Fig. 18. During measurements the 200 cm signal fiber is coupled to a 150 cm connectorized single-mode STF. These two fibers are from here on referred to as test fiber (STF tip acts as probe). Two measurements are made with this setup, the first without any liquid on the glass slide and the second with a drop of deionized water on the slide. The low-coherent signal wavelength of the reflectometer chosen for this setup is 1310 nm.

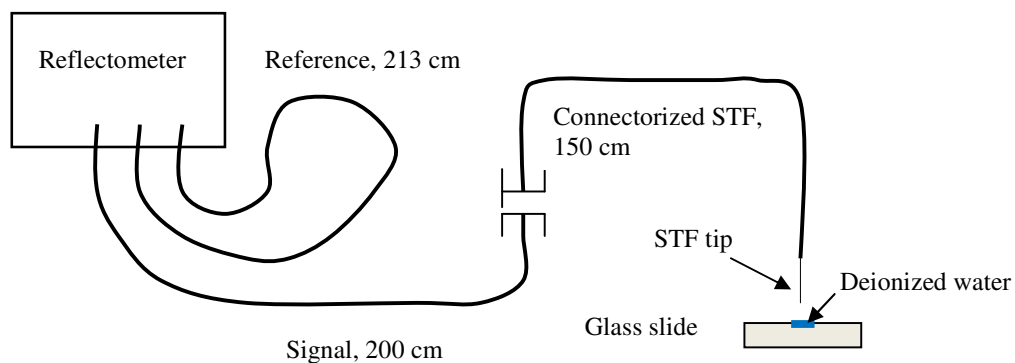


Figure 18: Setup for preliminary microfluidics studies.

Figs. 19a and 19b illustrate measurements made during the experiment for the microfluidics preliminary study. In both Figs. 19a and 19b it is possible to detect the reflection of the STF tip, which is the first peak on the left and with a signal intensity of 30 dB above the noise floor. It is also worth noticing that in Fig. 19a, the top and bottom surfaces of the slide can be distinguished as the second and third reflection peaks. The distance between the absolute positions of the reflections reveals the thickness of the sample, measured to be ~ 0.98 mm. When applying deionized water to the setup an additional reflection of the water surface occurs, as seen in Fig. 19b. Notice also the amplitude drop of the reflection of the top surface of the glass slide due to the liquid present on the slide, resulting to partial index-matching. The reflections of the STF tip and the bottom surface of the glass slide remain unchanged when deionized water is applied. Notice, however, that both reflection of the sample top and bottom surfaces are slightly shifted to the right when liquid is added to the experiment setup.

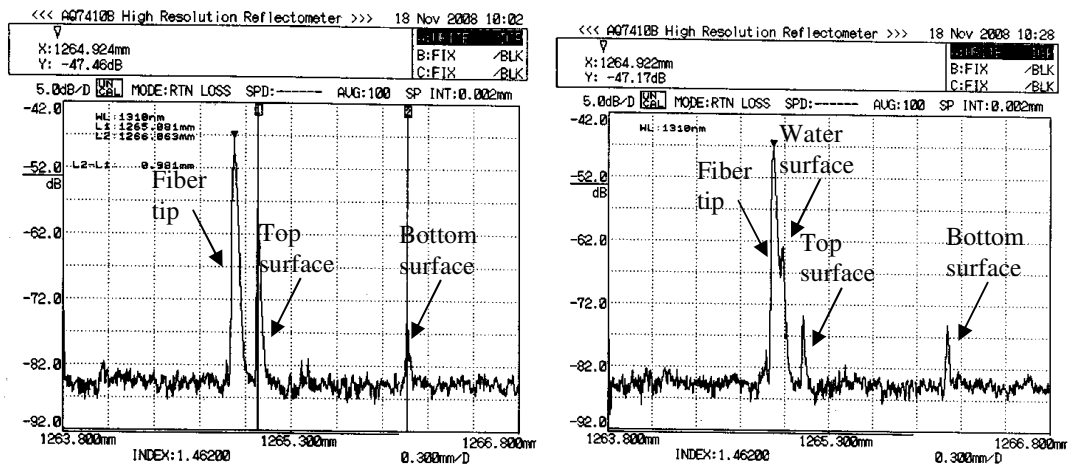


Figure 19: (a) Measurements made without water on the glass slide and (b) with water on the glass slide.

4.2.2 Results

The microfluidics preliminary study showed the possibility to use the reflectometer to detect the top and bottom surfaces of the glass slide, characterize its thickness and also detect the presence of liquid on the top surface of the slide. The results obtained from the preliminary study are helpful in the following experiments of combining the reflectometry measuring technique with fluid collection using the side-holes of a microstructured optical fiber. A special fiber arrangement is thus required for this purpose. It is worth mentioning that the STF used for the preliminary microfluidics study experiment did not have side-holes.

4.3 Microstructured fibers

An optical fiber with side-holes is required for the fluid collection experiments in order for the fiber to not only guide light but also to suck the liquid into the fiber. It is possible to combine optical fibers with different parameters, such as number of side-holes or fiber outer diameter, in order to obtain the optimal fiber arrangement for the application. Two of the fibers available for such experiments are illustrated in Fig. 20.

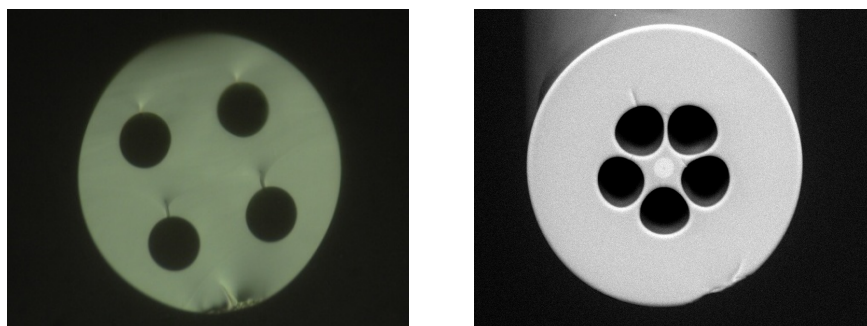


Figure 20: Two examples of fibers with side-holes used in this work. They are referred to as the 4-hole fiber (left) and the penta fiber (right).

When working with microstructured fibers for this type of application a number of aspects are to be considered. First, the optical fiber is required to guide the same amount of light through the entire fiber core. It is of interest to keep the losses of optical radiation as small as possible. Second, in order for liquid collection to be possible, the side-holes are required to be open not only in the collection side, but also in the remote side. Otherwise, the liquid cannot be sucked into the fiber. A method for opening the sides of a fiber with side-holes is needed if the remote end of the fiber is to be spliced to another optical fiber. For the present experiment, the fiber arrangement for liquid collection is to be optically connected to the signal fiber from the reflectometer. Therefore, it is necessary splicing the collecting fiber to a STF that is connectorized and coupled to the reflectometer. While a large number of side-holes make fluid collection more efficient, opening several side-holes from the side of the fiber to allow for fluid flow is complicated in practice.

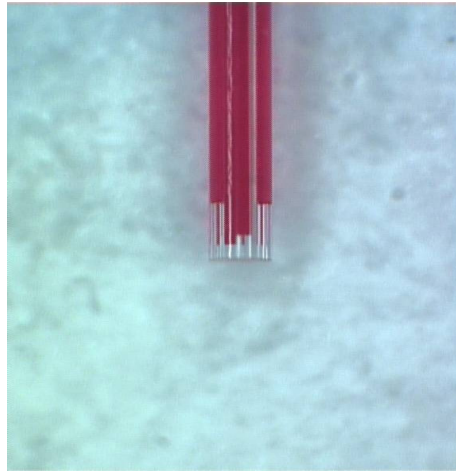


Figure 21: Illustration of collection of red liquid with a microstructured 4-hole fiber.

4.4 Four ways of allowing for flow

There are a number of ways to open the sides of a microstructured fiber to access the optical fiber side-holes. Four methods are introduced in this section. All four methods have advantages and drawbacks. The optical fiber chosen for the liquid collection part of the experiment is the microstructured fiber with four side-holes (see Fig. 21).

4.4.1 Polishing

In order to obtain four holes on the 4-hole fiber the optical fiber is polished where the distance to the side-hole is shortest. By rotating the fiber 90° and slightly shifting the position sideways each hole from different sides of the fiber is opened. This is a complicated method for preparing the fiber arrangement, and the handling time required is quite long. An advantage is that polishing does not affect the fiber core in any way, so the amount of light propagating through the optical fiber is not affected.

4.4.2 Fiber arrangement with capillary

The idea here is to combine an optical fiber with several side-holes with a capillary, and to splice the combination to a STF. Both the 4-hole and the penta fiber, see Fig. 20, are suited for this method. The thought is to polish the side of the capillary in order to access the liquid in the fiber, avoiding the need to side-polish each individual hole, as illustrated in Fig. 22. A problem with this combination is the large amount of light lost in the capillary, where there is no fiber core to guide the light. Although capillary sections as short as a fraction of a millimeter can be used, because of the need for high power light in the upcoming ablation experiments, the idea was discarded.

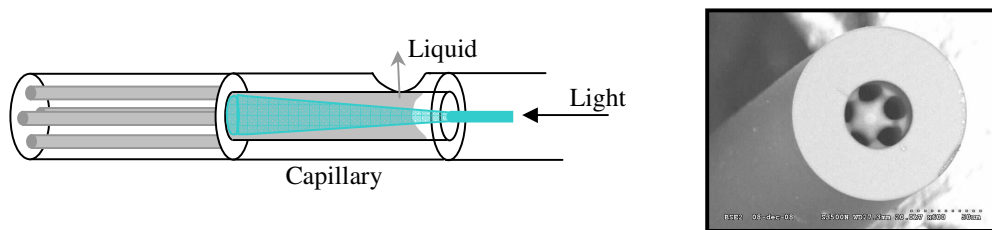


Figure 22: (Left) Setup for coupling all side-holes to a single capillary. The optical loss is estimated to be very high. (Right) SEM picture of a short capillary section ($<100\ \mu\text{m}$) spliced to a penta fiber.

4.4.3 Microexplosion

Another method for opening the sides of the 4-hole fiber is by heating the fiber on the position where the side-holes are to be open and adding pressure from inside. A microexplosion is then caused (see Fig. 23). Although the procedure takes a very short time to implement, a disadvantage is the possibility of the fiber core becoming damaged when opening the sides of the 4-hole fiber this way. When this method was tried and the optical fiber was illuminated with a HeNe laser, it was clearly seen that a great amount of light was coupled to the cladding where the sides had been opened. The measured loss of light through the optical fiber at a wavelength of 1310 nm is 23 dB, which is clearly a disadvantage. Another problem with this method is microbending, resulting in difficulties splicing the 4-hole fiber to other optical fibers.

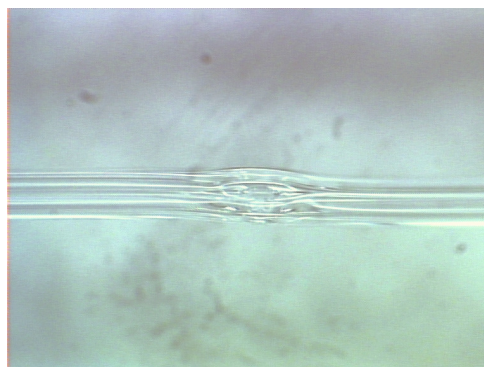


Figure 23: Image of four holes on the sides of a 4-hole fiber caused by microexplosion.

4.4.4 Optical fiber arrangement with an etched STF

Another solution for allowing fluid flow through a microstructured fiber is to maintain the microstructured optical fiber with side-holes intact and focus the processing on the STF. A possible method might be to etch a part of the STF, making thinner the end to be spliced to the optical microstructured fiber used for collection of liquid. The advantages of this method are that all cores are spliced minimizing losses and that etching a STF results in a more robust arrangement and requires less handling time than side-polishing a 4-hole fiber. Besides, with the use of optical fibers already drawn to smaller diameters (e.g., 80 μm), only a short (< 1 mm) spliced section of narrow fiber is required to allow for fluid flow through the side-holes, and etching can be avoided altogether. The drawback is that a small amount of light is lost due to another splice between fibers. The principle of the method is illustrated in Fig. 24.

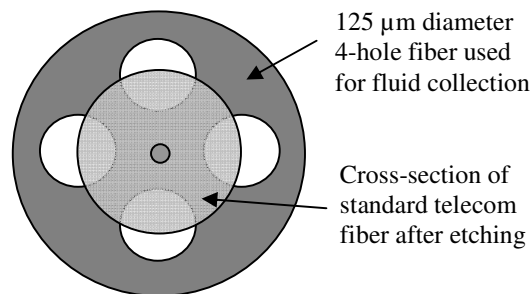


Figure 24: Front-view of a splice between microstructured fiber and etched standard telecom fiber that allows for good optical coupling and fluid flow.

For the fluid collection experiment it would have been possible to use a penta fiber instead of a 4-hole fiber. The penta fiber is a more appropriate microstructured fiber if working with smaller inclusions. However, the side-holes of a penta fiber are closer to the fiber core, so if polishing were to be used, a larger distance needs to be polished deep into the fiber, leaving it even thinner than a polished 4-hole fiber. If the microexplosion technique were to be employed, pressure and heating could damage the core of the fiber, since the distance to the side-holes of a penta fiber is small. However, it is possible to splice the microstructured 4-hole fiber to a penta fiber and use the five side-holes for collection of liquid. The openings of a penta fiber can be aligned so that the five holes of one fiber overlap with at least one of the four holes of the 4-hole fiber. In this way, there is an open way for all holes to lead fluid.

4.5 Final fiber arrangement

Various methods and fiber combinations have been discussed above for arrangement of a suitable optical fiber for the experiment, allowing light guidance and fluid flow. A possible fiber arrangement, which could also be considered to be the optimal arrangement, is to combine the 4-hole fiber with an etched STF. It is required to have an etched fiber that does not cover all of the side-holes entirely when spliced to the 4-hole fiber, as schematically shown in Fig. 24. Hydrogen fluoride, with a 50% concentration is used for etching the STF. A length of ~ 7 cm of the STF is etched for 15 min, resulting in

a fiber outer diameter of $\sim 78 \mu\text{m}$, which is sufficient for allowing proper splicing between the two optical fibers. The part of the STF that was not etched has still an outer diameter of $125 \mu\text{m}$ and can be easily spliced to other connectorized pieces of STF. The 4-hole fiber side-holes on the end spliced to the STF are not entirely closed. Hence liquid can be sucked into the fiber. The etched STF covers only half the radius of the 4-hole fiber side-holes.

With the HeNe laser it is possible to study the light propagating through both the 4-hole fiber and the etched STF, and to observe if light is lost in any part of the fiber when propagating through the fiber. This final optical fiber arrangement, seen in Fig. 25, is used for the upcoming experiment on combining low-coherence reflectometry and fluid collection.

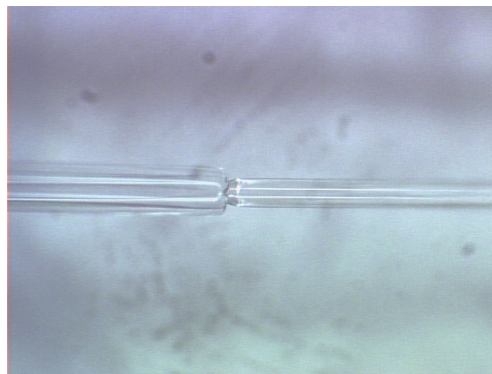


Figure 25: Image of ($125 \mu\text{m}$) 4-hole fiber spliced to an etched ($\sim 78 \mu\text{m}$) standard telecom fiber (STF).

4.6 Combining reflectometry with fluid collection

The purpose of this combined reflectometry and microfluidics experiment is to study fluid collection where the liquid is sucked into a microstructured optical fiber with side-holes, while monitoring the collection process with a reflectometer.

4.6.1 Setup

For the microfluidics and reflectometry experiment the single-mode fiber combination of a 4-hole fiber spliced to an etched STF is used. The experiment, which has the similar setup as illustrated in Fig. 18, consisted of approaching the tip of the fiber arrangement closer and closer to the liquid surface until contact is made between the fiber tip and the liquid, allowing for fluid collection. After some fluid is sucked into the side-holes, the fiber-liquid contact is broken. The steps of the experiment done are schematically illustrated in Fig. 26.

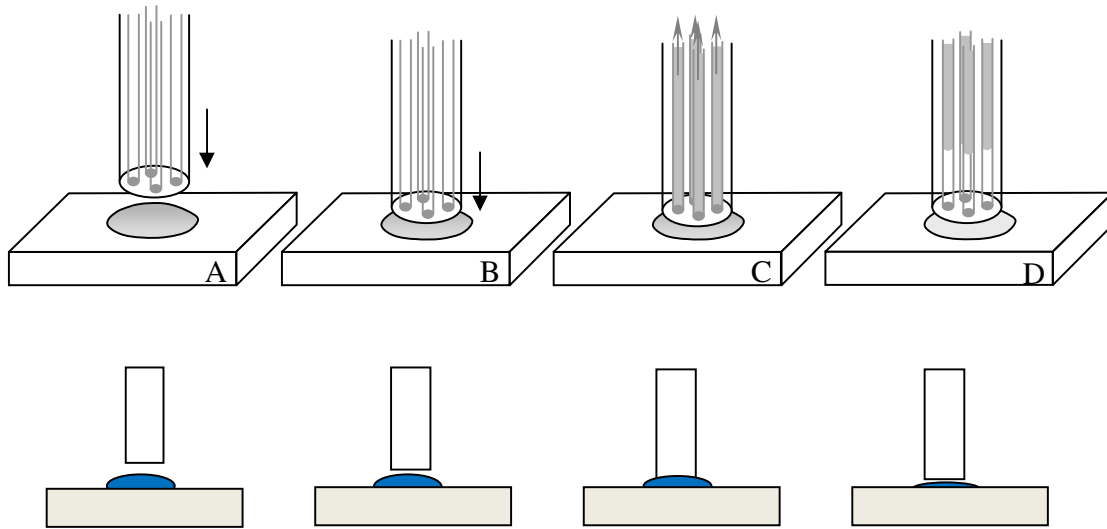


Figure 26: Illustration of each step of the liquid collection.

The first step of the combined low-coherence reflectometry and fluid collection experiment is to slowly approach the tip of the fiber arrangement to the liquid surface, as seen in Fig. 26a, and identify the reflections of the 4-hole fiber tip and of the liquid surface with the reflectometer. The reflection of the 4-hole fiber tip has a signal intensity of ~ 30 dB, which is a great amount of light reflected back through the fiber arrangement. The first peak to the left in Fig. 27a is due to reflection of the 4-hole fiber tip and the reflection next to the 4-hole fiber tip reflection is of the liquid surface. The distance between the fiber and liquid reflections is ~ 146 μm . By allowing the 4-hole fiber tip to approach closer and closer to the liquid surface the distance between the two reflection peaks decreases. The amplitude of the second reflection peak also changes, due to the increasing amount of light reflecting back from the water surface, as illustrated in Fig. 27b. The distance between the reflections is ~ 73 μm .

As the distance between the 4-hole fiber tip and the liquid decreases, shown in Fig. 26b, the reflectometer monitors the decreasing distance between the reflections, as seen in Fig. 27c. The distance continues to decrease slowly as the 4-hole fiber tip approaches the liquid surface, until the two independent reflection peaks can no longer be distinguished, resulting in only one reflection peak with greater amplitude, illustrated in Fig. 27d. It is worth mentioning that the 4-hole fiber tip is not in contact with the liquid yet, but the spatial resolution of the reflectometer (~ 20 μm) is insufficient to separate the two reflections. The moment the 4-hole fiber tip is in contact with the liquid (seen in Fig. 26c) the amplitude of the reflection drops, as illustrated in Fig. 27e. The amplitude drop is a result of index-matching. The drop in amplitude remains as long as the 4-hole fiber tip is in contact with the liquid. The position of the 4-hole fiber tip is remained unchanged and liquid is then sucked into the side-holes of the fiber. The amplitude of the reflection of the 4-hole fiber tip rises up again and a reflection of the liquid surface reappears (seen in Fig. 26f) when a part of the liquid has been collected into the fiber and the fiber-liquid contact has been broken, as illustrated in Fig. 26d.

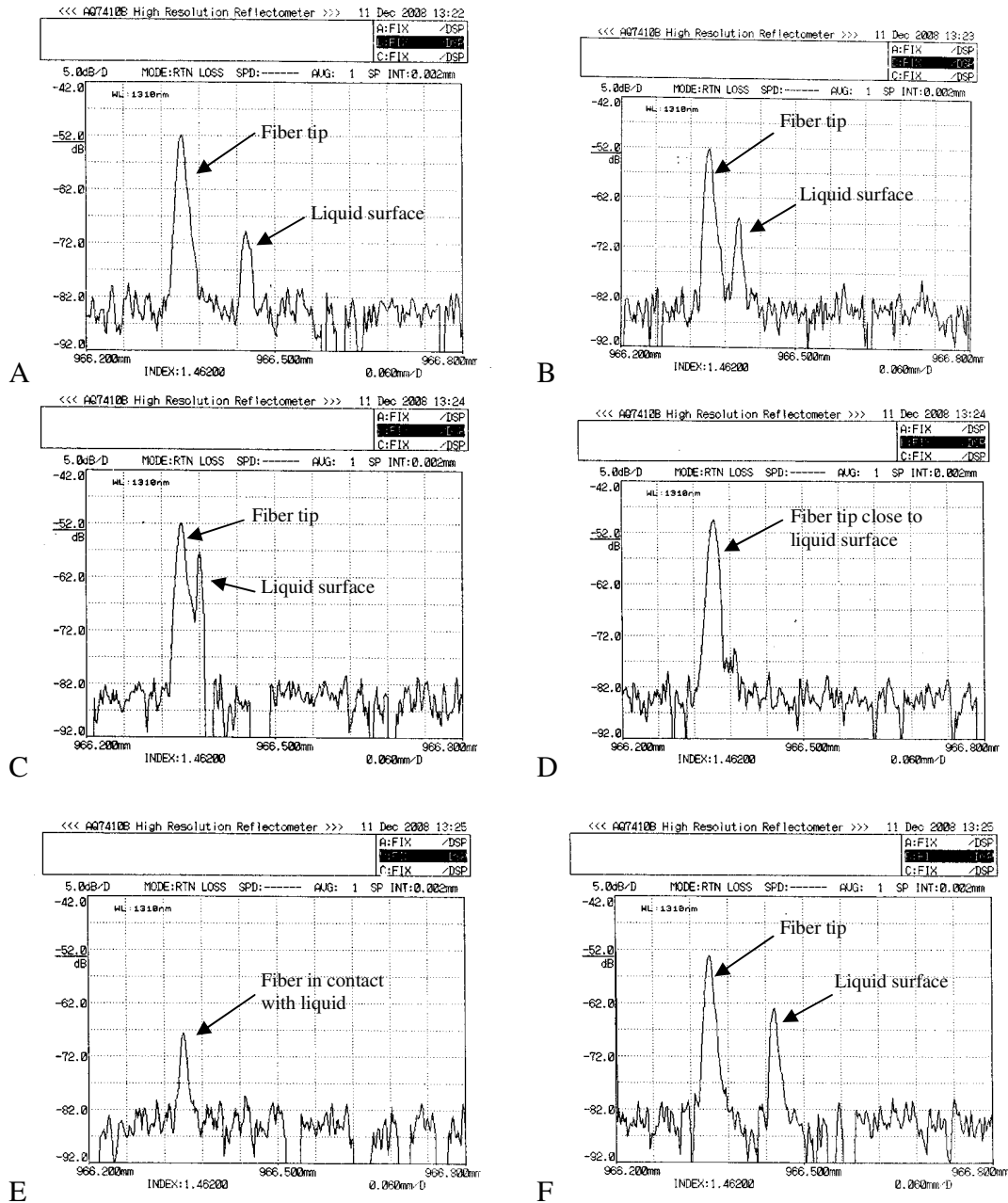


Figure 27: Each step of collection of liquid monitored with the high-resolution reflectometer.

It is not required to keep the 4-hole fiber tip in the same position when in contact with the liquid. The reflection of the fiber tip does not change when the position changes in liquid. If another reflection was observed while the fiber tip was still in contact with the liquid, the reflection peak could be identified as the reflection of the glass slide (top) surface. If the 4-hole fiber tip was not in contact with the liquid and a third reflection appeared (to the right of the liquid surface reflection), it indicated that the 4-hole fiber tip was close to the glass slide (top) surface.

4.6.2 Results

The experiment of combining fluid collection and low-coherence reflectometry clearly demonstrated that fluid collection in a microstructured fiber with side-holes, while monitoring the process with a high-resolution reflectometer, is possible. The next step is to combine both the fluid collection technique and low-coherence reflectometry with laser ablation. Laser ablation is to be discussed in the next section.

5 Laser ablation

5.1 Introduction to laser ablation

Laser ablation describes the process of removing material from a solid surface by irradiating the surface of the material with a laser beam. [16] At low laser flux, the material is heated by the laser energy and the surface of the material evaporates or sublimates. At high laser flux, a plasma is created which is partially ionized gas where some electrons are free rather than being bound to an atom or molecule. Laser ablation often refers to removing material with a pulsed laser, but ablation with a continuous wave laser beam is also possible if the laser intensity is high enough. The amount of material removed depends on the optical properties of the material and the wavelength of the laser. For the application considered here, it is advantageous to create an ablating plasma on the surface of the sample (e.g., bone or rock) without heating the sample too much. This is necessary to prevent destroying the liquid to be collected.

For ablation with pulsed lasers the pulses can vary over a wide range of duration, from femtoseconds to milliseconds, and can be precisely controlled making laser ablation interesting for both research and industrial applications. [17] There are some key parameters to consider when speaking of laser ablation. One parameter is to select a wavelength of operation, with a small absorption depth, to ensure a high energy deposition. Another parameter is the repetition rate. If the rate is too low, all of the energy not used for ablation will leave the ablation area and allow cooling. The quality of the beam is also an important parameter. The beam energy, determining the quality, cannot be fully used if it is not properly and efficiently delivered to the ablation area. If the size of the beam is not controlled the ablation area might be larger than desired.

5.1.1 Nd:YAG Laser

Lasers generate or amplify light. [18] Different types of lasers can amplify radiation at wavelengths ranging from the infrared to the ultraviolet region, and even to the X-ray regions. A pumping process is required in order to excite atoms into their higher quantum mechanical energy levels. For laser action to occur, the pumping process must produce a condition of population inversion, where more atoms are excited into a higher quantum energy level than there are in some lower level in the laser medium. The Neodymium-doped Yttrium Aluminum Garnet (Nd:YAG) laser can be operated both continuously and pulsed. However, different operating conditions require different laser designs. A continuously operating CO₂ laser generally requires different discharge conditions from a pulsed discharge. One important parameter is the control of the gas flow in order to obtain effective gas discharge. [19] For the laser ablation part of the diploma work a continuously operated Nd:YAG laser is used, with a wavelength of 1064 nm (infrared region). The laser is mode-locked and Q-switched at a repetition rate of 4.2 kHz with a pre-pulse of ~400 μs. Each individual 200 ps pulse is estimated at 40 kW.

5.2 Ablation of sample

5.2.1 Preliminary ablation study

The purpose of the preliminary ablation study is to investigate the parameters suitable for ablation of a material. The experimental setup for the ablation preliminary study is illustrated in Fig. 28. To avoid a diverging light beam, a lens is placed between the gold (Au) mirror and the sample, in order to obtain a better focus of the light beam. The distance between the lens and the sample is determined by the focal length of the lens. The samples used for the preliminary study of ablation are ~0.54 mm thin piece of silicon (Si) and a thin piece of aluminum (Al) foil. The thickness of aluminum foil is ~23 μm .

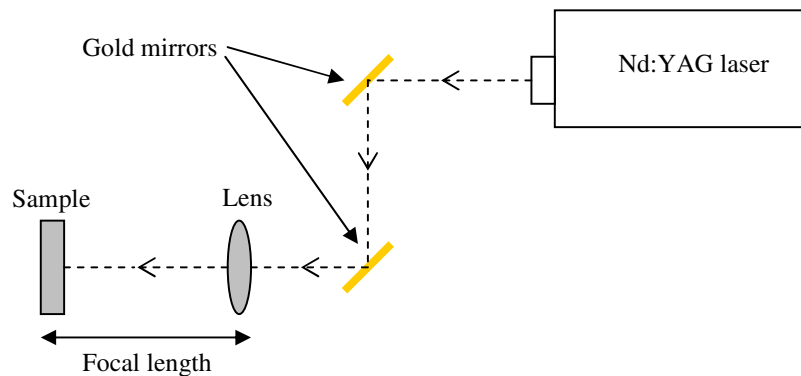


Figure 28: Experimental setup for preliminary laser ablation studies.

5.2.2 Results

Ablation through silicon is not possible with the Nd:YAG laser used for the experiment, due to the insufficient laser intensity. Another problem concerning the silicon sample is the amount of debris developed on the surface of the sample, due to the plasma created during ablation. The debris developed on the silicon sample is depicted in Fig. 29. A procedure is therefore required for removing the debris from the silicon sample surface. The main advantage with ablation of aluminum foil is the non-existing problem with debris on the sample surface. The ablated area is mostly smooth and homogeneous.

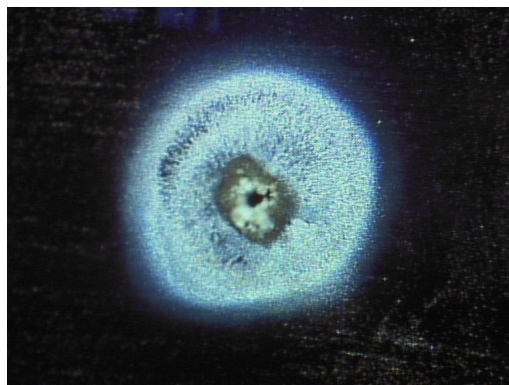


Figure 29: Ablated silicon with debris on the surface of the sample.

5.3 Ablation with an optical fiber combined with reflectometry

The results obtained from the preliminary study on ablation work as a foundation for the next experiment on ablation of aluminum foil with an optical fiber. During the ablation process the light is guided through the optical fiber and irradiates the aluminum foil surface, thus removing material from it. The ablation is to be monitored with the reflectometer. The ablation experiment consists basically of two parts. First part is to only study the ablation with an optical fiber. The second part is to combine laser ablation with low-coherence reflectometry, in order to study if ablation can be monitored with the reflectometer.

5.3.1 Setup part I

The setup for the first part of the experiment is quite similar to the setup for the preliminary study on ablation. The main difference between the two setups is the addition of the optical fiber. As seen in Fig. 30, the fiber is placed between the lens and the sample to be ablated, which in this case is a $\sim 23 \mu\text{m}$ thin piece of aluminum foil. The amount of average power coupled through the fiber is measured at the end of the optical fiber. It is possible to have an average output power of $\sim 600 \text{ mW}$ when using a STF, a laser repetition rate of 4.2 kHz and an operating wavelength of 1064 nm . The amount of average power, coupled through the fiber, sufficient for ablation with a setup with aluminum foil is $\sim 300 \text{ mW}$ (without a lens placed in front of the fiber tip). The Nd:YAG laser irradiates the aluminum foil sample for $\sim 1 \text{ second}$ and the sample is ablated. With the diverging beam, ablation is only possible with a distance $< 1 \text{ mm}$ between the probe and sample, before the intensity (per cm^2) becomes too small to ablate. A plasma plume develops during the ablation process and the plasma and debris ejected from the sample can possibly touch the back of the fiber tip and cause burning, which destroys the fiber and the ability to guide enough light. This can be avoided by not having the maximum average power coupled through the fiber ($\sim 600 \text{ mW}$) and by maintaining a distance between fiber tip and sample $> 50 \mu\text{m}$.

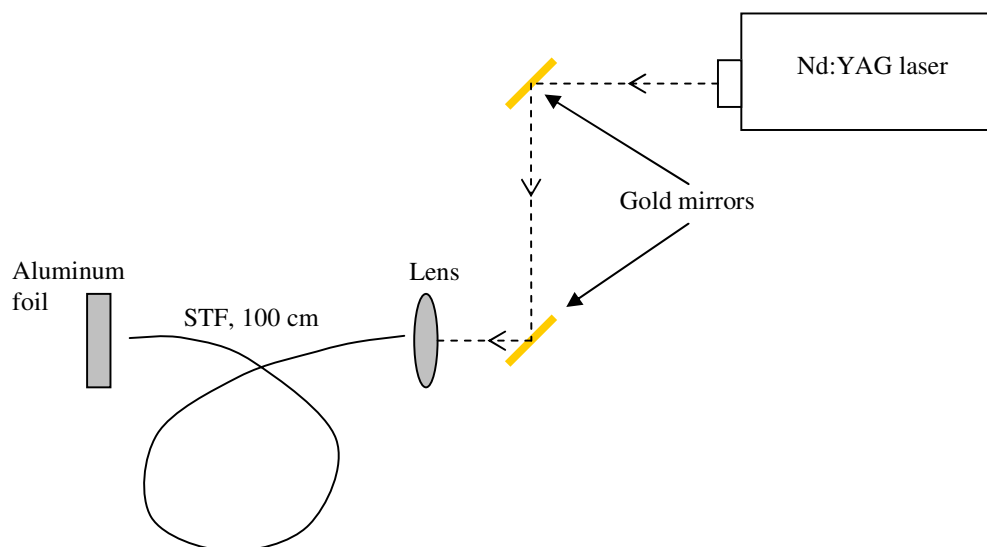


Fig.30: Experimental setup for ablation with an optical fiber

In Fig. 31 the size of the ablated area of the aluminum foil is compared to a STF (standard telecom fiber) with an outer diameter of 125 μm . The diameter of the ablated hole is estimated to be $\sim 60 \mu\text{m}$. For ablation of aluminum foil (using a lens) the average power coupled through the fiber is $\sim 80 \text{ mW}$. Therefore, aluminum foil is the sample to be used in upcoming ablation experiments with the reflectometer.

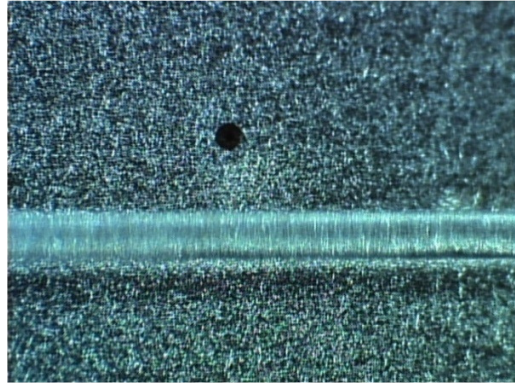


Figure 31: Ablation of a piece of aluminum foil. The size of the ablated area ($\sim 60 \mu\text{m}$) is compared to a STF with an outer diameter of 125 μm .

5.3.2 Setup part II

The ablation experiment with the previous setup demonstrated the parameters required for ablation of a thin ($\sim 23 \mu\text{m}$) sample of aluminum foil with an optical fiber. The next step is to monitor the process with the reflectometer. For the low-coherence reflectometry measurements one of the gold mirrors is removed as illustrated in Fig. 32. This prohibits light from the Nd:YAG laser to irradiate the sample and only guides the light from the reflectometer through the optical fiber. For alignment of the lenses in the current setup a HeNe laser coupled to a connectorized single-mode STF, is used as light source. An alignment is required for obtaining maximum amount of reflected light. After completed alignment, the connectorized STF is coupled to the 100 cm signal fiber of the reflectometer. The distance between the STF tip and sample can be adjusted with the help of the reflectometer. Note that the reference fiber of the reflectometer is now 313 cm. The additional length of reference fiber is due to a longer measuring distance.

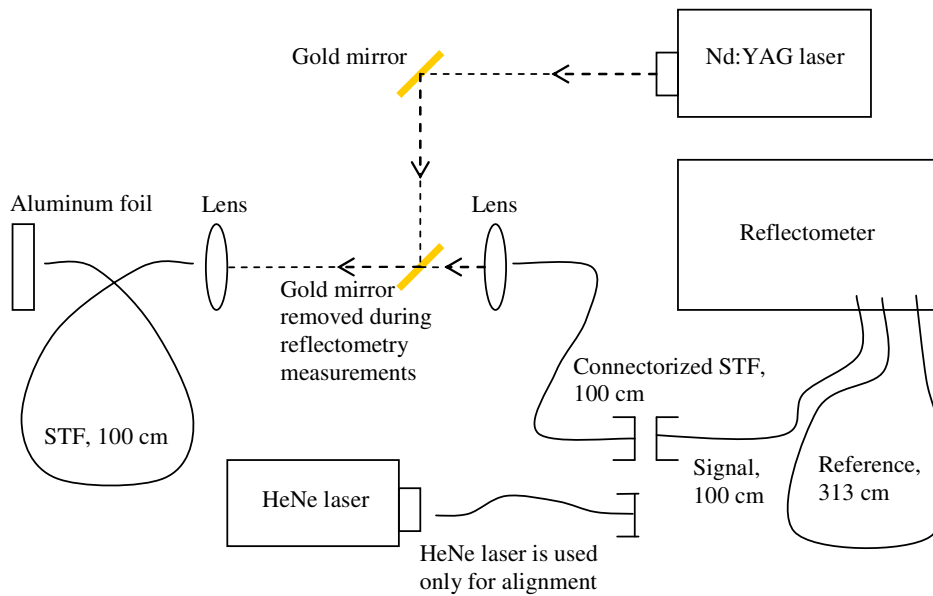


Figure 32: Experimental setup for ablation combined with reflectometry.

The reflections of both the STF tip and the aluminum foil sample are detected with the reflectometer. When approaching the aluminum foil sample with the STF tip, the absolute position of the sample reflection peak changes, and the distance between the two peaks decreases as the fiber tip is moved closer and closer towards the aluminum foil sample. When the distance between the reflections is $\sim 50 \mu\text{m}$ (illustrated in Fig. 33) the gold (Au) mirror is replaced in the setup, blocking the light from the reflectometer and allowing light from the Nd:YAG laser to ablate the aluminum foil sample.

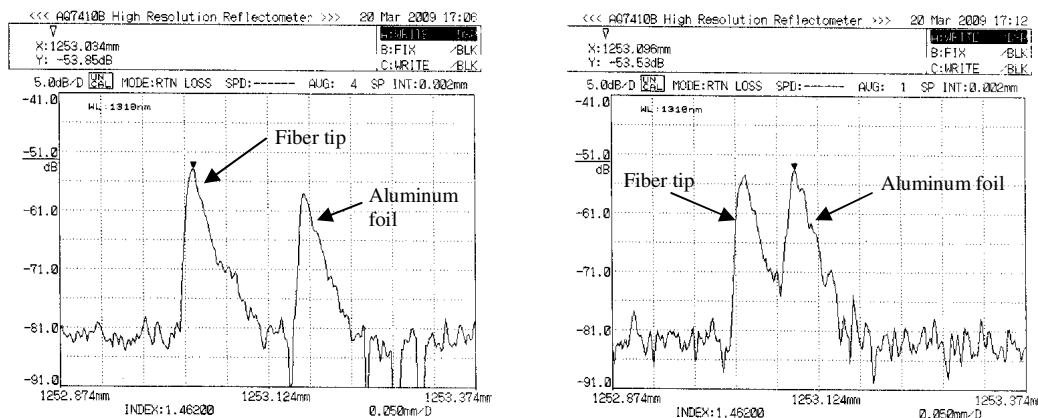


Figure 33: Illustrates the fiber tip approaching the aluminum foil sample for ablation, the distance between reflections are $150 \mu\text{m}$ (left) and $50 \mu\text{m}$ (right).

After a few seconds of ablation the mirror is removed again. Only the light from the reflectometer is then permitted. The measurements with the reflectometer illustrate a gradual decrease in amplitude of the aluminum foil reflection, which demonstrates the removal of aluminum foil due to ablation. The total decrease in amplitude of the aluminum foil reflection is $\sim 17 \text{ dB}$, seen in Fig. 34.

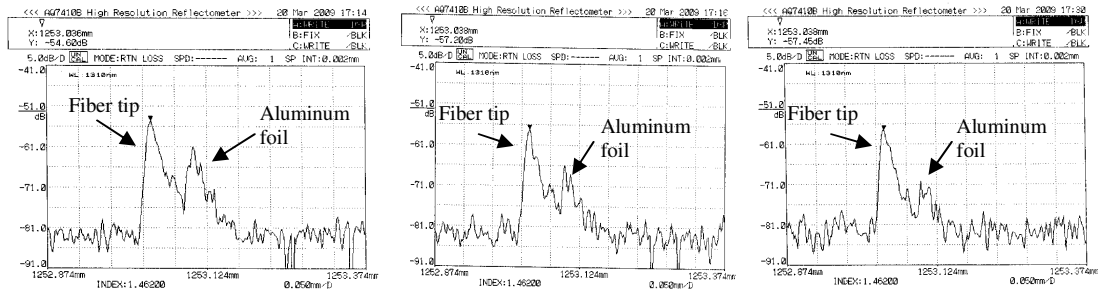


Figure 34: Illustration of the decrease of amplitude of the reflection peak of the aluminum foil during ablation.

5.3.3 Results

The experiments demonstrate that ablation with an optical fiber and monitoring the process with the reflectometer is possible. After ablation it is quite possible to have a damaged fiber tip, due to plasma and debris developed during ablation and ejected from the sample to the fiber tip. Debris on the fiber tip results in ‘glowing’ upon illumination. By measuring the power decrease on the output end of the fiber, it is possible to detect if the fiber has been damaged. The reflectometer could also detect a damaged fiber tip from the lack of reflection. To avoid this problem, it was experimentally found that the distance between the sample and the fiber tip should be $\sim 100 \mu\text{m}$ during ablation.

6 Combining reflectometry, ablation and fluid collection

The final step of the diploma work is to combine laser ablation, low-coherence reflectometry and fluid collection. The final experiment consisted of all the parts combined together and included the creating of an artificial system containing liquid (deionized water) with a surface of a piece of thin ($\sim 23 \mu\text{m}$) aluminum foil to be ablated. For simplicity, only a single-mode microstructured 4-hole fiber is used for liquid collection and not the fiber arrangement discussed in section 4.

6.1 Setup

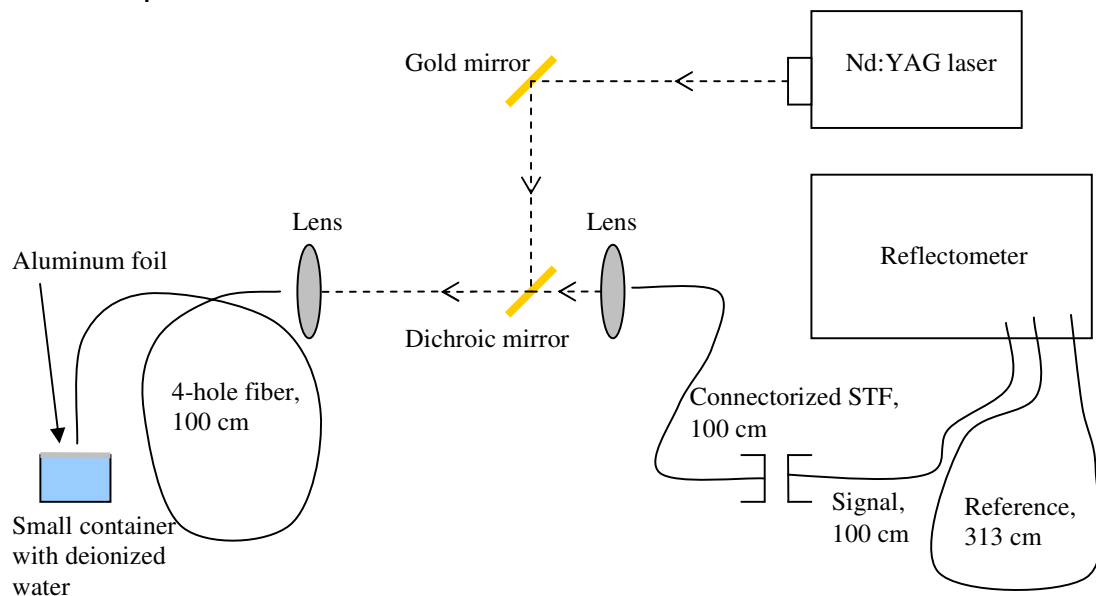


Figure 31: The experimental setup for combining low-coherence reflectometry, fluid collection and laser ablation.

The first step of the final experiment is to ensure that the reflectometer setup is correctly aligned. Thus an alignment procedure is required. Note that during alignment and measurements made with the reflectometer the light from the Nd:YAG laser is blocked (the dichroic mirror between the two lenses is never removed). The next step is to achieve the desired amount of average power through the optical fiber. An average power of ~ 500 mW coupled through the fiber (measured at the endface of the fiber) is sufficient for ablation of aluminum foil. The distance between the 4-hole fiber tip and the aluminum foil sample to be ablated is adjusted with the help of the reflectometer, illustrated in Fig. 32a. A distance of $\sim 100 \mu\text{m}$ between the aluminum foil and the 4-hole fiber tip will prevent a damaged fiber tip, but still allow for ablation to take place. The aluminum foil is then ablated for ~ 1 second. After ablation a reflection of the liquid surface appears on the reflectometer, illustrated in Fig. 32b. The 4-hole fiber tip is allowed to approach the liquid surface (seen in Fig. 32c) resulting in a decreasing distance between reflections of the liquid surface and the 4-hole fiber tip, until only a single reflection can be distinguished. The moment the 4-hole fiber tip is in contact with the liquid the single reflection peak drops, illustrated in Fig. 32d. Liquid is then sucked into the side-holes of

the 4-hole fiber. Take into account that for liquid collection, pumping in the liquid into the 4-hole fiber is not necessary, the capillary effect alone is sufficient for sucking liquid into the fiber. If the fiber-liquid contact is broken the reflection of the 4-hole fiber tip rises up again and the reflection of the liquid surface reappears (seen in Fig. 32f), thus resulting in completed liquid collection. It is also possible to break the fiber-liquid contact by moving the 4-hole fiber tip away from the liquid surface in order to complete the liquid collection process.

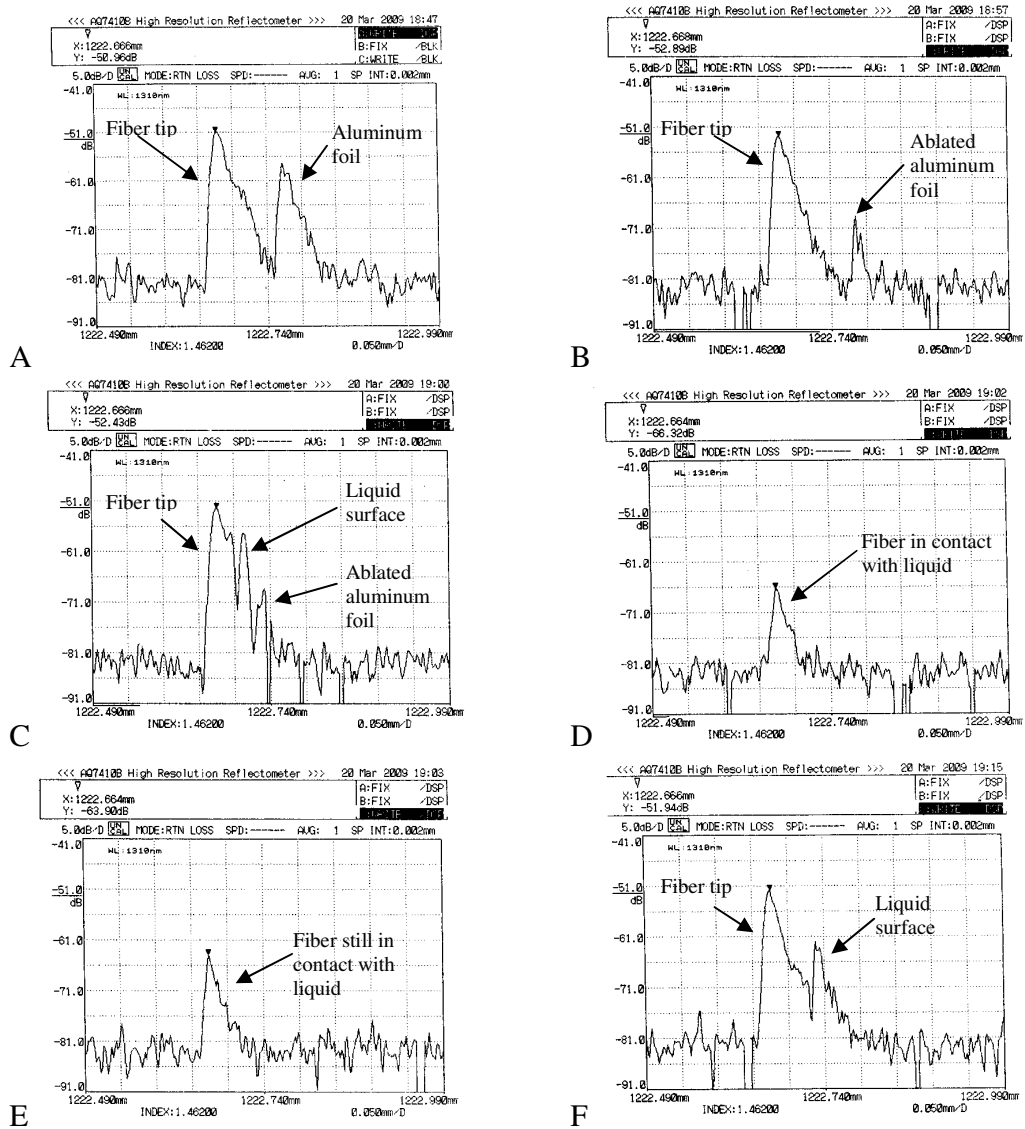


Figure 32: Schematically illustration of ablation and liquid collection, while monitoring the process with the high-resolution reflectometer.

6.2 Results

The experiment done demonstrates a successful combination of laser ablation and fluid collection, while monitoring both processes with low-coherence reflectometry, which was the aim with the diploma work. In the final experiment, the results obtained from the separate experiments worked as a foundation for the final combination of the three areas of ablation, microfluidics and reflectometry. The technique can be improved and refined for further studies on inclusions containing various types of fluids.

7 Conclusions and suggestions on future work

7.1 Conclusions

Conclusions, based on the experiments done and the results obtained, are stated below.

7.1.1 Reflectometry and fluid collection

The first, of three steps of this diploma work was to study the combination of fluid collection in a microstructured fiber arrangement, created solely for this purpose, with the aim to collect fluid while monitoring the positioning process with the reflectometer. The results obtained from the experiment show that the reflectometer can detect the fiber tip reflection, distinguish reflections of sample surfaces, and characterize sample thickness. It is possible, when allowing the fiber tip to approach a liquid surface closer and closer, to monitor with the reflectometer the decreasing distance between fiber tip and liquid reflections until the two become one single reflection peak, and when the fiber tip is in contact with the liquid surface observe the amplitude drop of the reflection, due to index-matching. All of this can be detected, measured and recognized with the reflectometer.

7.1.2 Reflectometry and laser ablation

The next step was to combine low-coherence reflectometry with laser ablation, with the goal to monitor the positioning for ablation of a material sample. A piece of a thin (~23 μm) aluminum foil was used as sample for this ablation experiment. The experiment showed that ablation through an optical fiber was possible. It was also possible to use the reflectometer to observe the ablation process. The reflectometer could detect a damaged fiber tip, by not obtaining a reflection.

7.1.3 Final combination

The final step was to combine the steps previously described in a single experiment and an artificial system was designed for liquid collection and ablation. The system consisted of a small container filled with colored deionized water and a thin (~23 μm) piece of aluminum foil on top of, to simulate a small inclusion. The results obtained from the final experiment demonstrated that the reflectometer monitored the positioning of the fiber tip for ablation, detected the aluminum foil surface and also detected (after completed ablation) the liquid surface. The liquid could be sucked into the side-holes of the fiber, due to the capillary effect, with only a 4-hole fiber. When the fiber-liquid contact was broken the reflection of the fiber tip increased again demonstrating completed fluid collection.

7.2 Further improvements on combining ablation and reflectometry

It is of interest to have a combined setup for ablation and low-coherence reflectometry which allows light guidance of both wavelengths 1310 nm and 1064 nm at the same time in a single optical fiber. Some of the methods to accomplish this are discussed below.

7.2.1 Use of coupler

The idea is to have a coupler in the setup, as schematically illustrated in Fig. 33, which guides light with wavelength of both 1064 nm and 1310 nm to the ablation area. When the light is reflected back the two wavelengths are separated by the coupler into two different optical fibers, one coupled to the Nd:YAG laser and the other to the reflectometer. The main disadvantage with this method is that the reflection peaks obtained with the reflectometer are very broad due to dispersion, resulting in measurements with bad accuracy. Another concern is the amount of reflected light from the Nd:YAG reaching the reflectometer. The small amount of light reflected back could possibly damage the reflectometer, or at least cause some disturbance to the reflectometry measurements.

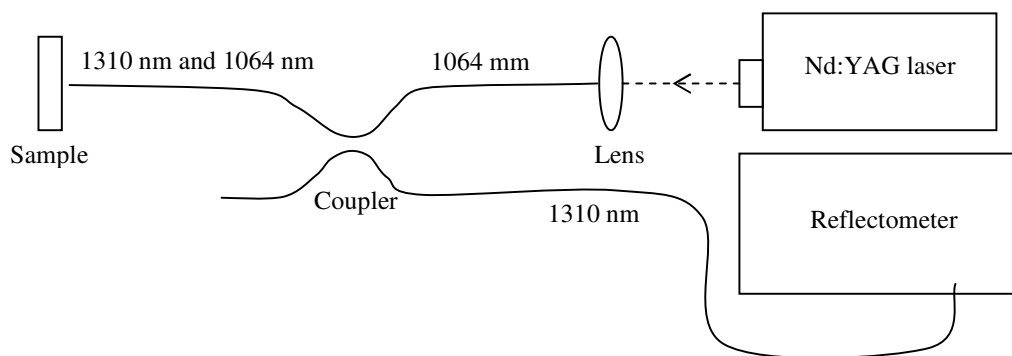


Figure 33: Illustration of adding a coupler to the final experiment setup.

7.2.2 Use of dichroic filter

Instead of having a gold mirror between the two lenses in the experiment setup, illustrated in Fig. 32, the mirror can be replaced with a dichroic filter, which allows light with a specific wavelength to pass but reflects light with another wavelength. The desired effect is to allow only light with a wavelength of 1310 nm to pass through the filter and to reflect the 1064 nm light, indicating that both the ablation and the low-coherence reflectometry measurements can take place at the same time. In practice, a small amount of reflected light with the wavelength of 1064 nm also passes through the filter. This is quite a huge disadvantage, thus the small amount of light is sufficient for interfering with the measurements made with the reflectometer or possibly damaging the reflectometer.

7.3 More efficient fluid collection

The final fiber arrangement used for the liquid collection, described in section 4.5, is further improved for a more efficient liquid collection as schematically illustrated in Fig. 34. The light from both the Nd:YAG laser and the reflectometer is guided through the STF and through the core of the 4-hole fiber for ablation and low-coherence reflectometry measurements. The fluid is then sucked into the side-holes of the 4-hole fiber and continuously flow into a 56 μm capillary, where the liquid can be collected and analyzed if needed. Basically the fiber arrangement separates the light and the liquid in the 4-hole fiber to two different optical fibers. Acreo is currently trying to patent this

fiber arrangement. Hence the details concerning the arrangement of the optical fibers cannot be discussed in this report.

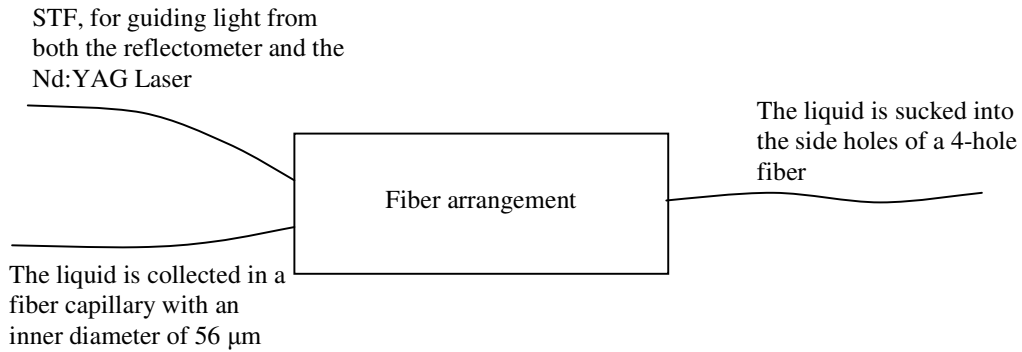


Figure 34: Illustration of a component for improved fluid collection, where the light guided through a STF continues in the core of the 4-hole fiber and liquid in the side-holes of the 4-hole fiber is transported to the fiber capillary.

8 References

- [1] Grattan K.T.V and Meggitt B.T. (1995), Optical Fiber Sensor Technology
- [2] http://en.wikipedia.org/wiki/Numerical_aperture
- [3] <http://www.tpub.com/neets/tm/106-9.htm>
- [4] <http://www.tpub.com/neets/tm/106-10.htm>
- [5] http://en.wikipedia.org/wiki/Plane_wave
- [6] <http://www.tpub.com/neets/tm/106-15.htm>
- [7] <http://www.tpub.com/neets/tm/106-14.htm>
- [8] <http://en.wikipedia.org/wiki/Polarization>
- [9] http://en.wikipedia.org/wiki/Fresnel_equation
- [10] <http://www.tpub.com/neets/tm/106-11.htm>
- [11] <http://www.tpub.com/neets/tm/106-12.htm>
- [12] Derickson D. (1998) Fiber Optic, Test and Measurement
- [13] http://en.wikipedia.org/wiki/Surface_tension
- [14] <http://en.wikipedia.org/wiki/Wetting>
- [15] http://en.wikipedia.org/wiki/Capillary_effect
- [16] http://en.wikipedia.org/wiki/Laser_ablation
- [17] <http://www.me.mtu.edu/~microweb/chap4/ch4-2.htm>
- [18] Siegman Anthony E. (1986), Lasers
- [19] Basting D. (1991) Industrial Excimer Lasers

Other literature

- Nordling C. & Österman J. (1999) Physics handbook